Power grid informed techno-economic analysis of the optimal PeWEC design

Energy 334 (2025) 137708

Contents lists available at ScienceDirect

Energy

journal homepage: www.elsevier.com/locate/energy

# Power grid informed techno-economic analysis of the optimal PeWEC design

Filippo Giorcelli [a,c,1], Enrico Giglio [a,b,c,1], Sergej Antonello Sirigu [a,c,*], Giuliana Mattiazzo [a,b,c]

[a] Department of Mechanical and Aerospace Engineering, Politecnico di Torino, Corso Duca degli Abruzzi 24, 10129, Torino, Italy
[b] Energy Center Lab, Politecnico di Torino, Via Paolo Borsellino 38/16, 10138, Torino, Italy
[c] Marine Offshore Renewable Energy Lab (MOREnergy Lab), Politecnico di Torino, Via Paolo Borsellino 38/16, 10138, Torino, Italy

ARTICLE INFO

*Keywords:*
Wave energy converters design
Energy system planning
Techno-economic optimisation
GA-MILP integrated framework

ABSTRACT

The role of ocean energy is expected to expand significantly in the coming years, driven by the need to meet the European Commission's SET Plan targets. Traditional wave energy converters (WECs) optimisation approaches prioritise minimising the Cost of Energy (CoE), but they often overlook grid integration challenges. However, mismatches between variable Renewable Energy Sources (vRES) production and actual grid demand arise due to factors like load shedding, storage limitations, and frequency requirements. This discrepancy is especially pronounced in off-grid systems with high vRES penetration. Therefore, it is crucial for WECs developers to consider the power grid's behaviour, ensuring that devices can generate electricity when it is most needed. This study examines the discrepancy between the wave energy cost derived from total energy production and that based on the energy actually delivered to the grid. The analysis examines WECs optimised solely for minimising the cost of energy alongside those which align with grid demand, emphasising the need to integrate grid information into the design process. Findings reveal a clear trade-off between devices that achieve optimal wave energy cost and those that minimise the Total Annual Energy System Cost (TAESC). Significant differences in operational continuity, curtailment, and power output are observed when comparing the device with the lowest CoE and the one with the best TAESC. This indicates that the economic viability of a WEC depends on designing a system capable of efficiently harnessing energy from the more frequently occurring, albeit less energetic, sea states rather than focusing solely on high-energy conditions.

## 1. Introduction

### 1.1. Background and problem statement

As the share of variable Renewable Energy Sources (vRES) grows, energy systems face increasing challenges in maintaining grid stability due to the intermittent nature of these technologies [1,2]. Energy scenarios are typically formulated to minimise overall energy costs while ensuring operational feasibility, including reserves and balancing requirements [3,4]. Therefore, accurate and cost-effective planning becomes especially critical in non-interconnected islands, where limited grid capacity and high vRES penetration exacerbate issues like load shedding, storage constraints, and curtailment [5,6].

In this context, energy planning plays a crucial role in ensuring a reliable transition pathway for policymakers. Effective energy planning models optimise the sizing of generation and storage technologies by also considering the technical characteristics of each, such as their capacity factor curves and specific capital and operational costs [7,8]. While established technologies such as photovoltaics (PV) and wind turbines (WT) power have relatively well-defined cost and performance metrics, early-stage technologies such as Wave Energy Converters (WECs) face greater uncertainty.

WECs offer valuable grid support by complementing solar and wind output and enhancing system flexibility, effectively mitigating renewable energy fluctuations [9,10]. They are particularly promising for non-interconnected islands, where wave resources are abundant and land is limited. Despite their promising attributes, WECs remain an early-stage technology. The ongoing technological divergence in their development complicates the identification of an optimal design or working principle, making it challenging to establish consistent cost and performance benchmarks for scenario optimisation [11,12].

Furthermore, current WEC techno-economic optimisation typically focuses on minimising Levelised Cost of Energy (LCoE)

* Corresponding author at: Department of Mechanical and Aerospace Engineering, Politecnico di Torino, Corso Duca degli Abruzzi 24, 10129, Torino, Italy.
*E-mail addresses:* filippo.giorcelli@polito.it (F. Giorcelli), enrico.giglio@polito.it (E. Giglio), sergej.sirigu@polito.it (S.A. Sirigu), giuliana.mattiazzo@polito.it (G. Mattiazzo).
[1] These authors contributed equally to this work as co-first authors.

https://doi.org/10.1016/j.energy.2025.137708
Received 18 April 2025; Received in revised form 4 June 2025; Accepted 21 July 2025
Available online 29 July 2025

## Nomenclature

### Acronyms

| | |
|---|---|
| AEP | Annual Energy Production |
| BESS | Battery Energy Storage System |
| CapEx | Capital Expenditure |
| ISWEC | Inertial Sea Wave Energy Converter |
| LCoE | Levelised Cost of Energy |
| NSGA-II | Non-dominated Sorting Genetic Algorithm II |
| PeWEC | Pendulum Wave Energy Converter |
| PV | Photovoltaic |
| TAESC | Total Annual Energy System Cost |
| WEC | Wave Energy Converter |
| BEM | Boundary Element Method |
| BFR | Ballast Filling Ratio |
| CoE | Cost of Energy |
| JONSWAP | JOint North Sea WAve Project |
| LVoE | Levelised Value of Energy |
| OpEx | Operational Expenditure |
| PTO | Power Take-Off |
| RAO | Response Amplitude Operator |
| vRES | variable Renewable Energy Source |
| WT | Wind Turbine |

### Variables

| | |
|---|---|
| q | WEC's state of motion vector |
| z | heave |
| $\epsilon$ | pendulum oscillation |
| A($\omega$) | added mass matrix |
| $f_\omega(\omega)$ | waves' excitation coefficients |
| $K_h$ | hydrostatic stiffness matrix |
| $a_\omega(\omega)$ | wave amplitude |
| $m_h$ | hull mass |
| $g$ | gravity acceleration |
| $I_p$ | pendulum moment of inertia |
| $l$ | pendulum arm length |
| $\tau$ | gearbox ratio |
| $c_{PTO}$ | damping control parameter |
| Occ | wave occurrences |
| L | WEC hull's length |
| H | WEC hull's height |
| h | WEC hull's bow-circumference ratio |
| $\alpha$ | WEC hull's draft parameter |
| $\psi$ | pendulum mass height |
| $N_u$ | number of pendulum units |
| $\rho_h$ | hull steel density |
| $\rho_b$ | ballast sand density |
| $N_{gen}$ | GA generation number |
| $f_{obj}^{base}$ | MILP objective function |
| $OC_{tot}$ | energy system's total operational costs |
| $t$ | time step |
| $\Omega_N$ | set of nodes $n$ |
| $\Omega_L$ | set of loads $l$ |
| $\Omega_S$ | set of storage system $s$ |
| $oc_{a,n}$ | operational costs of technology $a$ at node $n$ |
| $E_{s,n}$ | installed capacity of battery energy storage system $s$ at node $n$ |
| $d_{a,n,t}^{dsc}$ | electrical discharging of storage system $s$ at node $n$ and time instant $t$ |
| $f_{ln,t}$ | power flow in the $ln$-th line at time instant $t$ |
| $l_{l,n,t}$ | power demand at node $n$ and time instant $t$ |
| $\eta_{s,n}^{dsc}$ | discharge efficiency di storage system $s$ at node $n$ |
| $CF_{r,n,t}$ | capacity factor of RES $r$ at node $n$ and time instant $t$ |
| $T_{res}$ | pitch resonance period |
| $P_{WEC}$ | WEC nominal installed capacity |
| $p_{WEC}$ | hourly value of WEC's power produced |
| $\eta_{p_{WEC}}$ | WEC's conversion efficiency |
| $p_{0,WEC}^{tot}$ | annual maximum theoretically producible value of WEC's power |
| $x$ | surge |
| $\delta$ | pitch |
| M | mass matrix |
| B($\omega$) | radiation mass matrix |
| $\omega$ | frequencies |
| $K_p$ | pendulum stiffness matrix |
| $T_{PTO}$ | PTO torque |
| $m_p$ | pendulum mass |
| $I_h$ | hull moment of inertia |
| $d$ | distance between WEC's centre of gravity and pendulum oscillation axis |
| $T_{ctrl}$ | applied control torque |
| $k_{PTO}$ | stiffness control parameter |
| $N_w$ | non-zero occurrent waves |
| $P_{abs}$ | WEC's average absorbed power |
| W | WEC hull's width |
| Dr | WEC hull's draft |
| k | WEC hull's height-draft ratio |
| $\phi$ | pendulum mass width |
| $l_p$ | pendulum mass length |
| $\lambda_0$ | pendulum unit position |
| $\rho_p$ | pendulum mass density |
| $N_{ind}$ | GA population size |
| $y_{25}$ | WEC's operational lifetime |
| $CC_{tot}$ | energy system's total capital costs |
| $w_t$ | time step weight |
| $\Omega_t$ | time interval |
| $\Omega_{LN}$ | set of lines $ln$ |
| $\Omega_R$ | set of RES $r$ |
| $cc_{a,n}$ | capital costs of technology $a$ at node $n$ |
| $P_{a,n}$ | installed capacity of technology $a$ at node $n$ |
| $d_{a,n,t}$ | electricity output of technology $a$ at node $n$ and time instant $t$ |
| $d_{a,n,t}^{ch}$ | electrical charging of storage system $s$ at node $n$ and time instant $t$ |
| $K_{ln,n}$ | network's incidence matrix |
| $e_{s,n,t}$ | state of charge di storage system $s$ at node $n$ and time instant $t$ |
| $\eta_{s,n}^{ch}$ | charge efficiency di storage system $s$ at node $n$ |

| | |
|---|---|
| $P_{r,n}$ | installed generation capacity di RES $r$ at node $n$ |
| $E_{BESS}$ | BESS energy installed capacity |
| $\hat{p}_{WEC}$ | normalised WEC's power produced in one hour |
| $p^{max}_{WEC}$ | maximum annual value of WEC's power produced in one hour along a year |
| $p_{0,WEC}$ | maximum theoretically producible hourly value of WEC's power |

without adequately considering grid integration, possibly leading to energy surpluses, increased curtailment, and underutilised generation [11–14] This mismatch can result in Total Annual Energy System Cost (TAESC) higher than initially predicted by optimisation models, particularly when excessive storage is required to absorb surplus production. In contrast, devices with slightly higher CoE that generate energy more closely aligned with load curves could result in a lower TAESC by better matching energy production with grid demand.

### 1.2. Literature review

#### 1.2.1. Techno-economic optimisation of WEC design

Despite more than a century of development, WEC technology has not yet converged on a dominant design, reflecting its lower maturity compared to other offshore renewable technologies. This limited commercialisation is primarily due to the wide range of operating principles, deployment options (onshore, offshore, nearshore), and strong dependence on local climatic conditions [11].

Optimisation efforts typically aim to improve individual device performance using technical, economic, or techno-economic metrics [12, 13,15]. However, as noted by Guo and Ringwood in [12], these efforts are often fragmented due to the complexity of modelling wave energy systems and the absence of standardised performance metrics or optimisation process. Notably, maximising Annual Energy Production (AEP) alone does not guarantee the economic viability of a WEC. As a result, a range of performance metrics has been proposed as objective functions, which can be broadly classified into three categories: technical (78%), techno-economic (14%), and economic (8%) [12].

The LCoE is widely recognised as a central metric, though less applicable in early-stage development where alternative metrics like displaced mass, installed power or capital expenditure per AEP are used [16–18]. Multi-objective optimisation frameworks are also employed to capture trade-offs between cost and performance [19]. Besides, bottom-up methods have been developed to estimate LCoE in the absence of commercial-scale deployments. These methods have proven effective in reducing the risk of inaccurate cost estimation for technologies still in the early stages of development [20].

Research also point out the relevance of geometry optimisation [12, 13], and calls attention to manufacturability and reliability [21–23]. Some authors advocate for interdisciplinary approaches involving also policy and economic perspectives to evaluate investment risks of WECs projects [24]. Notably, [14] stress out to the absence of frameworks linking WEC design with grid integration, as well as approaches capable of accounting for ancillary benefits that WECs could offer to an energy system beyond conventional metrics like LCoE.

#### 1.2.2. Technology design driven by energy planning model

Recent literature highlights the need to align WEC design with grid behaviour and system-level performance. Traditional WEC optimisation, focused on maximising energy capture, fails to capture the economic value of generation timing and system compatibility [25].A more comprehensive approach should include grid-aware optimisation with the contributions of the complete portfolio of involved technologies and subsystems, *e.g.* vRES and Battery Energy Storage Systems (BESS) [26].

Energy planning models, commonly formulated as Linear or Mixed-Integer Linear Programming (LP or MILP), optimise installed capacities to minimise system-wide costs while ensuring that the power system meets demand [27,28]. These models require input productivity curves, which are relatively straightforward for PV and WT but more complex for WECs due to the diversity of device architectures [29].

Integrating WECs with offshore wind and BESS has shown to improve power predictability, smoothes output, and reduce curtailment [30]. Meanwhile, [31] emphasises the importance of evaluating WECs not only in terms of their LCoE but also their Levelized Value of Energy (LVoE), which captures the correlation between energy production and market prices.

McCabe et al. [32] introduce a system-level optimisation approach for WECs, using energy planning models to inform the weighting of techno-economic and environmental objective functions. Their framework defines metrics that incorporate avoided costs of energy, which reflect system-wide economic benefits resulting from the ability of wave energy to reduce the need for eventual investments in generation, storage or transmission to meet the demand along the year [33]. In addition, they incorporate avoided environmental costs of energy [34], which capture the positive environmental impacts resulting from the substitution of non-renewable sources with renewable ones. These savings may also include reductions in total system costs through optimised renewable energy portfolios [35]. In their work, they do not evaluate specific device geometries but instead focuses on formulating and proposing a multi-disciplinary framework. Accordingly, the complementary seasonal production profile of wave energy for specific sites, as demonstrated in a study of California's 2045 zero-carbon energy goals, highlights its potential to cost-effectively supplement solar and wind energy, despite higher installation and maintenance costs [36].

Further studies on hybrid systems for isolated communities highlight the value of integrated planning. In [37], although WEC design is not incorporated into the energy system optimisation process, the inclusion of grid-related metrics like curtailment and storage requirements is shown to significantly inform decision-making. Moreover, [38] examines the integration of wave farms into isolated grids, addressing real-time stability and equipment wear, but without exploring scenario-based planning or WEC design optimisation.

### 1.3. Proposed solution and contribution

While the literature increasingly acknowledges the need to evaluate WECs from a power system perspective, to the best knowledge of the authors no studies directly investigate optimal WEC design impact to system-level metrics under varying planning scenarios. Existing work tends to either optimise WECs in isolation or explore energy planning without design-specific feedback.

Although lacking in the literature, integrating scenario-based energy planning into the WEC optimisation process could allow for a more robust evaluation of device performance under varying system conditions, such as different levels of renewable penetration and storage capacity.

Therefore, this work proposes an integrated methodology that simultaneously evaluates WEC design and its impact on energy system planning. By simulating multiple WEC design configurations within a representative energy scenario, the approach quantifies how device characteristics influence not only the energy production but also broader techno-economic performance of the overall energy system. To the best of the authors' knowledge, this represents the first effort to bridge detailed physical modelling of a WEC with scenario-based energy system planning optimisation. The framework is particularly relevant for non-interconnected islands, where the alignment of renewable generation with demand is critical to achieving cost-effective, resilient energy systems.

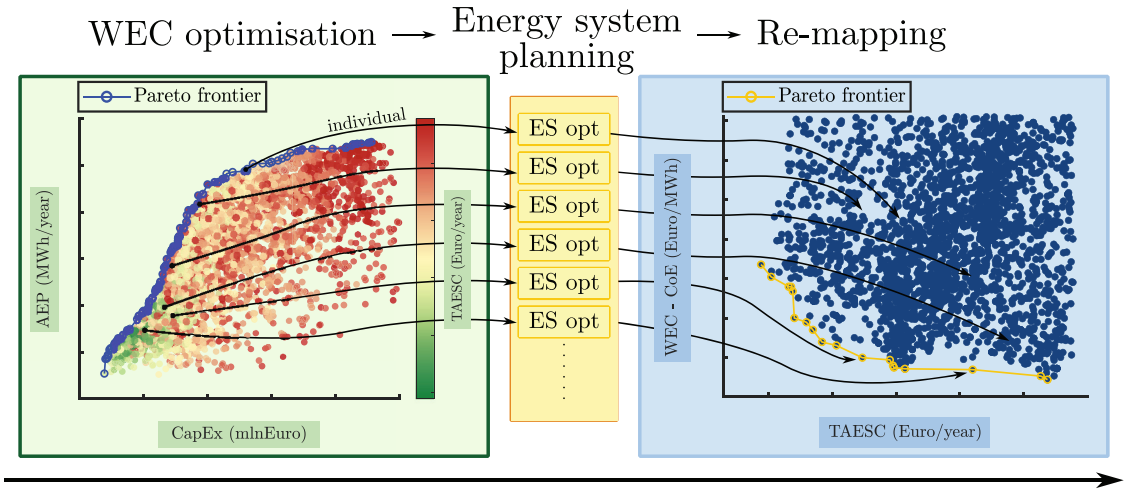


**Fig. 1.** Schematisation of the proposed novel integrated framework.

### 1.4. Structure of the work

The reminder of the paper is organised as follows. In Section 2 the methodology employed in the present study is comprehensively presented. In Section 2.1 the procedure chosen to identify a set of WEC optimal designs is reported, together with a focus on the chosen WEC architecture and its working principle (Section 2.1.1), the main governing equations (Section 2.1.1.1) and the numerical model (Section 2.1.2). Afterwards, in Section 2.2 the details on energy system planning model are given. Section 3 presents the case of study, while Section 4 delves into a complete analysis and discussion of the results. The main conclusive remarks are at last reported in Section 5.

## 2. Methodology

This study focuses on the development of a novel method to support the decision-making phase in the optimal design selection of WECs by considering both the techno-economic optimisation of the device and its integration into a defined energy system. The proposed approach represents an integrated methodology that simultaneously evaluates WEC design and its impact on energy system planning. Although applied here to a specific case study, the framework is general and adaptable to other contexts by changing the WEC archetype, location-specific parameters, and energy system model.

In the preliminary phase, a multi-objective optimisation of the WEC design is conducted independently from the energy system. The optimisation framework aims to simultaneously minimise the Capital Expenditure (CapEx) of the device and maximise its AEP. This process, based on design space exploration via a genetic algorithm (GA), produces a dataset of potential design configurations, with the dominant solutions forming the Pareto frontier [39]. Given the early-stage nature of the technology, a simplified techno-economic parameter is introduced instead of the LCoE, specifically the Cost of Energy (CoE), which is calculated as the CapEx over AEP ratio:

$$\mathrm{CoE} = \frac{\mathrm{CapEx}}{\mathrm{y}_{25}\mathrm{AEP}} \tag{1}$$

where $\mathrm{y}_{25}$ is the operational life of the device, considered to be 25 years in this work, consistent with previous literature [19].

In the second phase, each WEC design from the initial dataset is integrated into the energy system model. An energy system optimisation is then performed for each individual configuration, with the objective of minimising the TAESC. This enables a comprehensive assessment of the broader system-level implications of each design solution. By linking component-level design to system-level performance, the methodology provides a new CoE–TAESC mapping (Fig. 1), resulting in a refined Pareto front that captures the trade-off between device-level cost-effectiveness and system-wide performance.

The described methodology is broadly applicable to other scenarios. The approach offers a valuable foundation for further investigations into energy system-aware WEC design optimisation and supports the development of co-design strategies for renewable energy technologies and energy systems.

In the following subsection, each step of the proposed methodology is introduced in detail. In particular, the WEC design optimisation and dataset generation are contextualised using a selected WEC archetype. However, as previously mentioned, the approach remains general and can be applied to other WEC devices and energy systems by appropriately adapting the relevant models and site-dependent parameters.

### 2.1. WEC design optimisation via GA stage

#### 2.1.1. The PeWEC device & working principle

Among the various WECs designs proposed in the literature, this study focuses on the Pendulum Wave Energy Converter (PeWEC) device, developed at the Marine Offshore Energy Lab of the Politecnico di Torino in collaboration with the National Agency for New Technologies, Energy, and Sustainable Economic Development (ENEA). The PeWEC has been chosen as a representative case study due to its unique technical features and the presence of well-established theoretical and applied research [40–42]. Furthermore, extensive experimental investigations and numerical model validations have laid a solid foundation for its development [43,44]. The PeWEC was specifically developed for deployment in the Italian Mediterranean Sea, making it an ideal candidate for the case study of the island of Ustica, which is presented in this work. Fig. 2 shows the render and a 3D-CAD section of the full-size device, describing the internal WEC components schematisation.

The PeWEC is a pitching floating WEC that exploits the pendulum working principle to harvest the wave energy. A sketch of the device, its reference systems, working principle and degrees of freedom is given in Fig. 3. The pitching motion of the hull, induced by incoming waves, excites the pendulum rotation around its axis ($\varepsilon$), which is connected via a gearbox to a permanent magnet synchronous motor [40]. All conversion systems are housed within a sealed hull, rendering the PeWEC a fully enclosed system. This design enhances the WEC's reliability by completely isolating critical components of the energy conversion mechanism from the hostile marine environment. The device's station-keeping is achieved through four mooring lines specifically engineered to withstand severe sea state conditions while enabling pitching motion during operational scenarios.

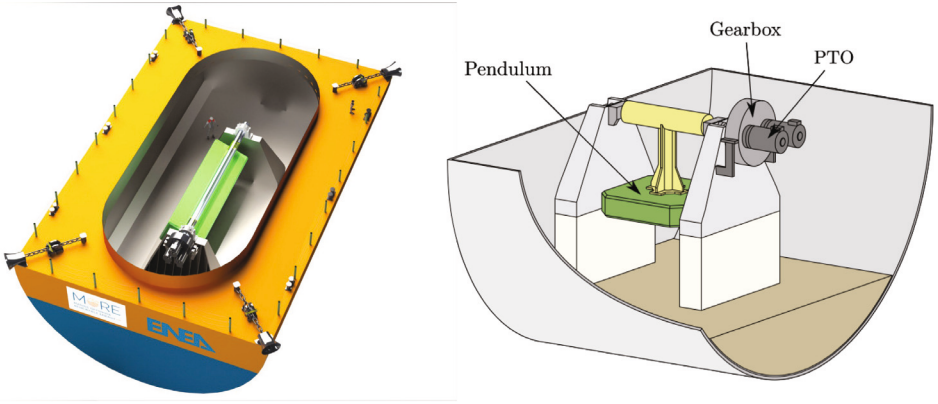


**Fig. 2.** On the left, full-size PeWEC render. On the right, a 3D section describing the internal WEC components schematisation.

*2.1.1.1. Governing equation and model.* The use of a techno-economic optimisation framework requires the adoption of numerical models that are both fast and accurate in evaluating the productivity of the WEC, and, in this specific case, the PeWEC. For this reason, a state-of-the-art linear frequency domain modelling approach has been adopted in this work [19,45]. Therefore, the hydrodynamic interactions are evaluated under the potential-flow theory assumptions, *i.e.* constant mean wetted surface, while both irrotational and incompressible flow [46,47].

Considering the WEC to be self-oriented with respect to the incoming wave, only mono-directional waves oriented with the longitudinal axis of the hull are assumed. Therefore, it becomes reasonable to describe the state of motion of the device (q) with a vector of 4 components, called: surge (x), heave (z), pitch ($\delta$), and pendulum oscillation ($\varepsilon$):

$$\mathrm{q} = \begin{bmatrix} \mathrm{x} & \mathrm{z} & \delta & \varepsilon \end{bmatrix}^{\mathrm{T}} \tag{2}$$

The fundamental mathematical equations governing the dynamics of the PeWEC system can be formally introduced as:

$$[\mathrm{M} + \mathrm{A}(\omega)]\ddot{\mathrm{q}} + \mathrm{B}(\omega)\dot{\mathrm{q}} + [\mathrm{K}_h + \mathrm{K}_p]\mathrm{q} = a_\omega(\omega)\mathrm{f}_\omega(\omega) + \mathrm{T}_{\mathrm{PTO}} \tag{3}$$

where M is the mass matrix, $\mathrm{K}_h$ is the hydrostatic stiffness matrix, $\mathrm{K}_p$ is the pendulum stiffness matrix, $a_\omega(\omega)$ is the wave amplitude, and $\mathrm{T}_{\mathrm{PTO}}$ is the Power Take-Off (PTO) torque. The linear frequency domain model equation is solved by means of potential flow theory [48], thus obtaining the hydrodynamic curves for the waves' excitation coefficients $\mathrm{f}_\omega(\omega)$, added mass $\mathrm{A}(\omega)$, and radiation damping $\mathrm{B}(\omega)$. The frequency dependent variables $\mathrm{A}(\omega)$, $\mathrm{B}(\omega)$, $\mathrm{f}_\omega(\omega)$ and $\mathrm{K}_h$ are evaluated for a set of representative frequencies via a Boundary Element Method (BEM) solver software called NEMOH [49]. The coupling between the hull and the enclosed pendulum-based electro-mechanical system is described by the contributions of the inertial and pendulum restoring forces, expressed in M and $\mathrm{K}_p$ as [19,50]:

$$\mathrm{M} = \begin{bmatrix} (m_h + m_p) & 0 & m_p(d-l) & -m_p l \\ 0 & (m_h + m_p) & 0 & 0 \\ m_p(d-l) & 0 & I_h + I_p + m_p(d-l)^2 & I_p + m_p l^2 - m_p dl \\ -m_p l & 0 & I_p + m_p l^2 - m_p dl & I_p + m_p l^2 \end{bmatrix} \tag{4}$$

$$\mathrm{K}_p = \begin{bmatrix} 0 & 0 & 0 & 0 \\ 0 & 0 & 0 & 0 \\ 0 & 0 & -g m_p(d-l) & g m_p l \\ 0 & 0 & g m_p l & g m_p l \end{bmatrix} \tag{5}$$

The hull mass is denoted by $m_h$ and $g$ is the gravity acceleration. The hull and pendulum moment of inertia are reported as $I_h$ and $I_p$, respectively. The masses of pendulum is described as $m_p$. Then, $d$ and $l$ are the distances between WEC's centre of gravity and pendulum oscillation axis and pendulum arm length ($\overline{\mathrm{GA}}$ and $\overline{\mathrm{PA}}$, respectively, shown in Fig. 3).

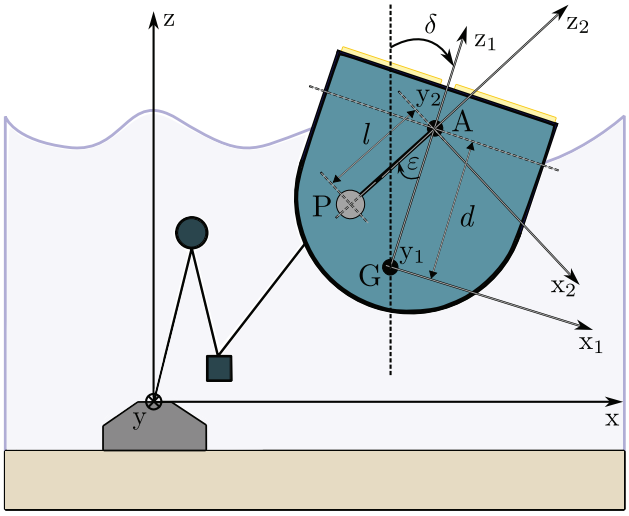


**Fig. 3.** Schematic representation of PeWEC device and its working principle, with relative coordinates references systems.
*Source:* Adapted from [40]

In order to exploit the wave energy harvesting, a energy maximiser control system based on a reactive proportional-derivative control law is designed to be employed for the PTO regulation. The applied control torque ($\mathrm{T}_{ctrl}$) acts both as a reactive component and a damping with respect to the pendulum rotation around its axis and therefore the absorbed power will have a negative sign. Moreover, considering also the gearbox ratio $\tau$, the PTO torque would be expressed as part of the control torque dynamic matrix:

$$\mathrm{T}_{\mathrm{PTO}} = \begin{bmatrix} 0 & 0 & 0 & \mathrm{T}_{\mathrm{PTO}} \end{bmatrix}^{\mathrm{T}} \tag{6}$$

Concerning the control scheme actuated on the PeWEC's PTO, the strategy employed is the so-called reactive control, as already done in [50]. The control torque is formulated as a linear combination of rotational velocity and rotation around the pendulum oscillation axis by means of two parameters which mimic a stiffness ($k_{PTO}$) and a ($c_{PTO}$) contribution:

$$\mathrm{T}_{ctrl} = -k_{PTO}\varepsilon - c_{PTO}\dot{\varepsilon} \tag{7}$$

The two control parameters are optimised with respect to a set of representative simulated sea states, in order to maximise the extracted power, checking a posteriori if the constraints set by the mechatronic system have been overcome and dismissing the pairs of control parameters that do not meet such thresholds, *i.e.* generator rotational speed

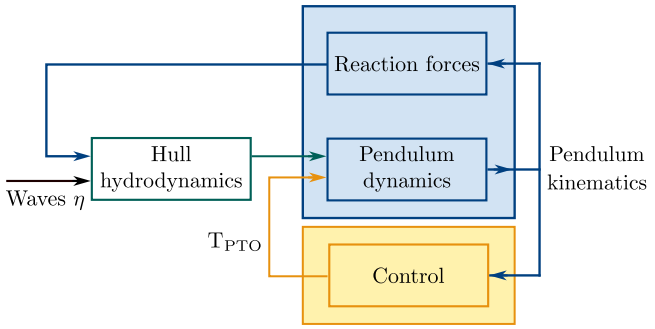


**Fig. 4.** PeWEC block diagram. The wave forces, acting on the hull, generate the pendulum unit motions which discharge its loads on the hull and it is regulated by the control system.

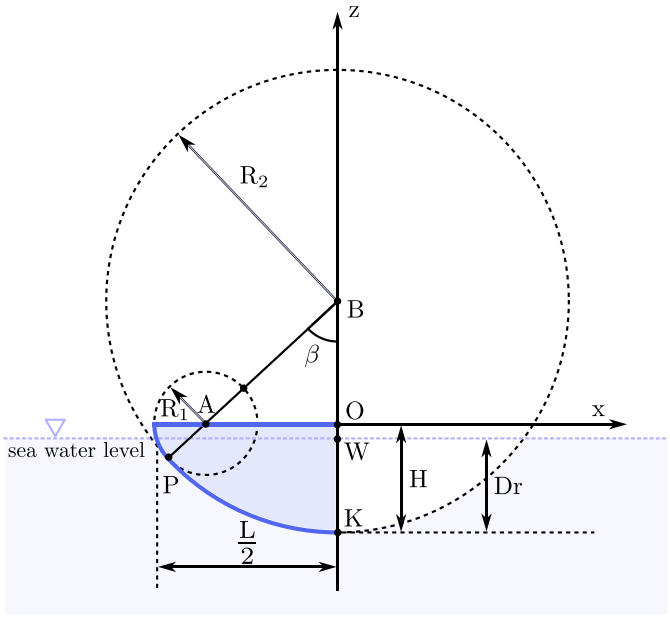


**Fig. 5.** PeWEC's hull profile description on the x-z plane.
*Source:* Adapted from [19]

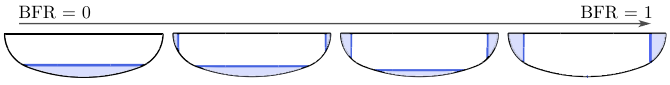


**Fig. 6.** Effect of BFR on the ballast inertia allocation.

must not exceed the rated speed while the PTO torque must not exceed the nominal one.

A couple of optimal control parameters $(k_{PTO}^{opt}, c_{PTO}^{opt})$ is evaluated for each sea state of the set of simulated waves, which are modelled according to a JOint North Sea WAve Project (JONSWAP) spectrum [51,52] and chosen as representative for the analysed site. Finally, the AEP is computed as:

$$\mathrm{AEP} = \frac{3600 \cdot 24 \cdot 365}{100} \sum_{j=1}^{N_w} \mathrm{Occ}_j^{\%} \mathrm{P}_{abs}^{j}(k_{PTO}^{j,opt}, c_{PTO}^{j,opt}) \tag{8}$$

where $j$ is the index of each of the $N_w$ waves with non-zero occurrence $\mathrm{Occ}_j^{\%}$, to which correspond a $\mathrm{P}_{abs}^{j}(k_{PTO}^{j,opt}, c_{PTO}^{j,opt})$ average absorbed power if the set of $(k_{PTO}^{j,opt}, c_{PTO}^{j,opt})$ control parameters is employed.

As previously assumed in the aforementioned study [19], in order to maintain the numerical model linear (and thus computationally cost-effective) further assumptions concerning the numerical model have been made with regard to the neglect of drift and second-order forces, mooring, and viscous damping effects. However, even in this study, it is worth to mention that validation of the present model is, nevertheless, ensured by further experimental studies, which ensure adequate accuracy and representativeness of the results for the techno-economic purposes of the study carried out [43,44]. In Fig. 4 is shown the block diagram representing the PeWEC numerical model.

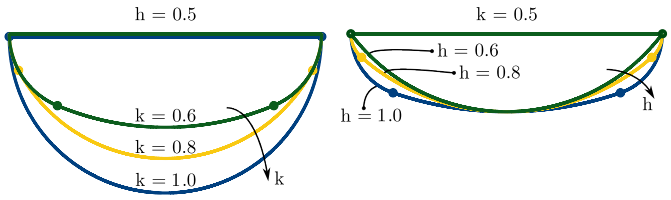


**Fig. 7.** Influence of increasing k (on the left) and h (on the right), respectively with the other parameter fixed.

### 2.1.2. Techno-economic optimisation framework

Similar to the study conducted by Sirigu et al. [19], each PeWEC device is fully parametrised by a set of 13 design parameters (6 for the hull, 6 for the pendulum unit and 1 for the PTO) that significantly influence the WEC's performance and associated costs.

*2.1.2.1. Device parametrisation.* The hull shape of the PeWEC is built relying on prior development experience capable to balance manufacturability, reliability and hydrodynamic performances [19]. The device's profile section on the x–z plane features a curve described by a bottom circumference which is tangential to two other circumferences (at the bow and stern, respectively). The floater is symmetric with respect to the y–z and x–z planes and is formed by extruding the hull's profile along the $y$-axis. The complete geometrical description of the PeWEC's profile is reported in Fig. 5.

In the geometrical scheme, the following relevant dimensions characterising the hull are reported:

- the device semi-length, L/2;
- the PeWEC height, defined as the total WEC's size along the $z$-axis, H;
- the draft of the hull, Dr;
- the radius of the first and second circumferences, $R_1$ and $R_2$;
- the angle $\beta$ forming by ◁PBO.

Then, from the geometrical parametrisation of the hull, it is possible to extrapolate the subset of design parameters completely describing the device's hull:

I. the hull length L, which is the total WEC's size along the $x$-axis;
II. the hull width W, which is the total WEC's size along the $y$-axis;
III. the hull shape parameter h, related to the bow-circumference ratio ($h=\frac{x_A}{L/2}$);
IV. the hull height parameter k, related to the device's height-draft ratio ($k=\frac{H}{Dr}$);
V. the hull draft parameter $\alpha$, which defines a limiting pitch angle under operating conditions to prevent excessive green water sloshing on the device deck. From $\alpha$ is derived the device draft (Dr) as $Dr = H - \frac{L}{2}\tan\alpha$;
VI. the Ballast Filling Ratio (BFR), which describe the ballast allocation among aft/fore and keel tanks. The BFR is formulated as the ratio between the ballast located in the stern and bow ballast tanks and the total WEC's ballast (*i.e.* it is comprised between 0 and 1). The effect of progressively increasing the BFR on the ballast inertia distribution is illustrated in Fig. 6.

The influence of geometric parameters h and k on the hull's profile are shown in Fig. 7.

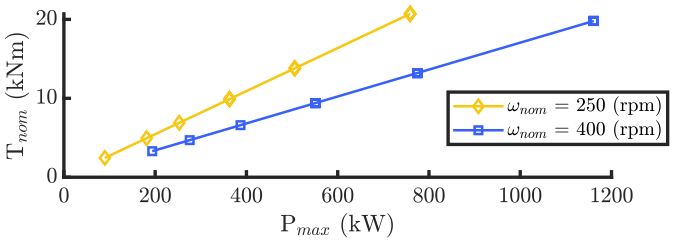


**Fig. 8.** Combination of nominal speed and torque for the deployable PTO systems.

As a major driver of WEC's costs and performances, the device's masses and inertia are conveniently parametrised. Based on previous experiences in the Inertial Sea Wave Energy Converter (ISWEC) design, the present work assumes the floater's structural mass $m_h$ to be 130 times the total device's volume and its walls to be treated as thin plates. Therefore, an equivalent structure thickness is computed using the total surface of the floater and $m_h$. A standard naval carpentry steel has been chose as material employed to build the hull, with a density $\rho_h$ of 7800 kg/m$^3$. Instead, the considered ballast material is sand, with density $\rho_b$ of 1400 kg/m$^3$ and a convenient cost-specific weight ratio.

The WEC's pendulum-PTO unit is fully defined via the remaining seven design parameters:

VII. the pendulum mass $m_p$,
VIII. the pendulum arm length - l,
IX. the pendulum mass width - $\phi$,
X. the pendulum mass height - $\psi$,
XI. the number of pendulum units - $N_u$,
XII. the unit position - $\lambda_0$,
XIII. the PTO ID.

The pendulum unit mass $m_u$ is determined by adding a mass housing coefficient (40% in percentage terms) to the pendulum mass $m_p$ in order to incorporate the pendulum's support structure, the PTO and the gearbox.

The pendulum unit consists of a steel parallelepiped mass (density of $\rho_p$ = 7800 kg/m$^3$) with dimensions $\psi$ x $\phi$ x $l_p$, positioned at a distance l from the pendulum's fulcrum. The pendulum mass $m_p$ and its dimensions are among the six design parameters of the pendulum unit. The length $l_p$ can be easily calculated through geometric considerations. The height of the pendulum fulcrum is defined by the unit position design parameter $\lambda_0$, which allows the full swinging rotation of the pendulum mass around its fulcrum.

Finally, for the conversion stage, a PTO system is employed, consisting of a permanent magnet synchronous motor for each pendulum, coupled with an appropriately selected gearbox designed for high-torque and low-speed operating conditions. In the PeWEC parametrisation, the final design parameter is the PTO ID, which defines a specific PTO system from a catalog of 37 different options. Each PTO-ID is characterised by a combination of nominal speed, gearbox ratio and torque values, as shown in Fig. 8.

The 13 PeWEC's design parameters are listed in Table 1. The reported lower and upper bounds over which the optimisation algorithm will research for the convenient PeWEC design, have been set based on the previous author's experience and ensure a proper design variation.

Starting from the 13 design variables, the framework proceeds with the geometrical characterisation of the device and parametrisation of the pendulum unit. Once the device is fully identified, the hydrodynamic problem is solved by means of the implementation of a BEM solver software (NEMOH [49] in this case) and thereby the dynamic responses of the system to wave forces are calculated. Then, the inner optimisation loop is performed in which the two aforementioned parameters ($c_{PTO}$ and $k_{PTO}$) representing the stiffness and damping of the PTO, are properly tuned by applying the presented control logic in order to maximise the energy extraction from the pendulum motion for each simulated sea states. This optimisation loop is repeated for each PeWEC design explored. Finally, the AEP of the device is calculated taking into account the marine energy resource for the selected site of installation.

**Table 1**
GA's free variables for the definition of a singular individual.

| Parameter | Unit | Lower bound | Upper bound |
|---|---|---|---|
| Hull length - L | (m) | 10 | 30 |
| Hull width - W | (m) | 5 | 25 |
| Hull shape ratio - h | (/) | 0.4 | 1 |
| Hull height ratio - k | (/) | 0.4 | 1 |
| Hull draft parameter - $\alpha$ | (/) | 15 | 25 |
| Ballast filling ratio - BFR | (/) | 0.1 | 1 |
| Pendulum mass - $m_p$ | (kg) | 5000 | 30 000 |
| Pendulum arm length - l | (m) | 0.5 | 5 |
| Pendulum mass width - $\varphi$ | (m) | 0.5 | 2.5 |
| Pendulum mass height - $\psi$ | (m) | 0.45 | 2.5 |
| Number of pendulum units - $N_u$ | (/) | 1 | 4 |
| Unit position - $\lambda_0$ | (/) | 1 | 1 |
| PTO ID | (/) | 1 | 37 |

**Table 2**
Overview of WEC's CapEx major drivers considering the case study presented in [20].

| Driver | Unit | Relative cost |
|---|---|---|
| PTO | (€/kW) | 1297 |
| Electronic components | (€/kW) | 2000 |
| Pendulum unit | (€/kg) | 7.30 |
| Hull | (€/kg) | 8.15 |
| Mooring + Installation (including electrical cable) | (%) of total WEC cost | 36 |

In addition, it has opted to also install PV modules on the deck of each of the PeWECs (elements in yellow in Fig. 3) deployed in the sea during the scenario simulation, in order to take advantage and exploit the new space generated by the devices without going to further stress the already scarce amount of available land onshore. The characteristics of the PV panels installed on the WECs present dimensions of 2.4 m $x$ 1.3 m with a size of 700 W (already used in [53]). For the computation of the total amount of modules that can be installed on each deck, we referred to an occupancy coefficient of the total deck area of 50%.

*2.1.2.2. Device costs.* Concerning the formulation of the device costs, in this work we refer to the cost functions derived from the bottom-up approach described in [20]. The major drivers considered in the CapEx evaluation are: hull costs (dependent on the mass of the structure and thus the cost of material, including also accessories costs), PTO costs (related to the typology and size of the PTO), mechanical component costs (*i.e.*, pendulum, basement, shaft, and joints including assembly costs), electronic component costs (function of the WEC power size), mooring and installation costs (assumed as a percentage addition to the total system's cost, including also marine cable installation and set equal to 30%). Although absolute costs remain uncertain, the resulting cost parametrisation of each device's subsystem is presented in Table 2 for the case of study analysed in [20], highlighting the important cost's drivers during optimisation.

The limited operational experience with long-term offshore WECs plants prevents a reliable estimation of their Operational Expenditure (OpEx) [54]. Operation and maintenance costs depend on both WEC-specific factors and external conditions. Key WEC characteristics which affect OpEx include the adopted archetype, operating principle, device size, and susceptibility to failure [55]. External factors include inter-annual resource variability at the installation site, frequency of extreme events, maintenance strategy (corrective or preventive), the adopted chosen repair scheme, and the learning rate deriving from the sector experience [56–58]. In the literature, OpEx is typically estimated as a percentage of the total system cost or CapEx [54,57–59], suggesting values between 1.4% and 7%. Also in this study, OpEx is defined as a fixed share (5%) of the total cost and included in the CapEx evaluation.

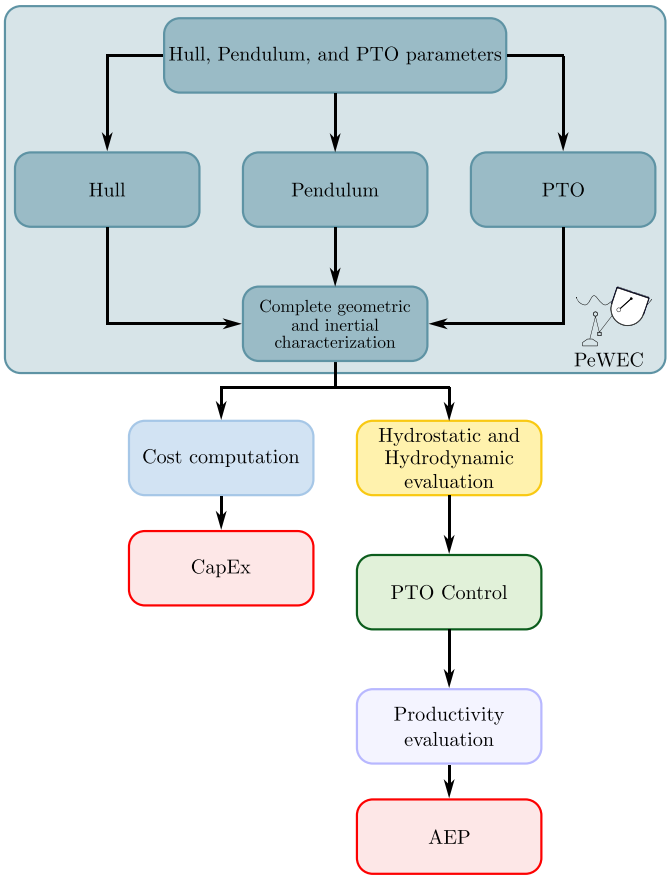


**Fig. 9.** Block chart schematisation of the PeWEC model.

This accounts for 35% of the total WEC cost, encompassing mooring, installation (including the marine cable), and OpEx, aligning with the data presented in the case study in Table 2. Therefore, only CapEx is explicitly considered.

As mentioned above, due to the early stage of their technological industrialisation, WECs could result in a not cost-effective energy source with respect to other more mature technologies. However, motivated by the high potential of wave energy, ambitious target have been set worldwide, supported by different proactive and trustful plans aimed at reducing the cost of energy for WECs.

Different reports suggest to follow cost-reduction pathways based both on promising technological aspects [60,61] and the development of a innovative ecosystem for sustainable and competitive growth of WECs, *i.e.* exploiting the implementation of new policies, financial supports, continues innovation actions, and niche markets evolution [62–64]. Therefore, referring to the possible techno-economic projections developed in the aforementioned researches, in the present work are assumed:

- a 50% reduction in the PeWEC's actual CapEx, considering an escalating installed capacity and an increasing learning rate of the PeWEC industrialisation process [62,65,66],
- a 100% increase in the AEP, in accordance with the advancing maturity of the technology's performances compared with the suboptimal control law used in this work for the preliminary assessment of productivity, *e.g.* by the implementation of optimal advanced control strategies [67,68].

*2.1.2.3. GA framework.* Fig. 9 shows the block outline of the steps performed by the numerical model of the WEC under analysis to assess the objective functions of the optimisation problem.

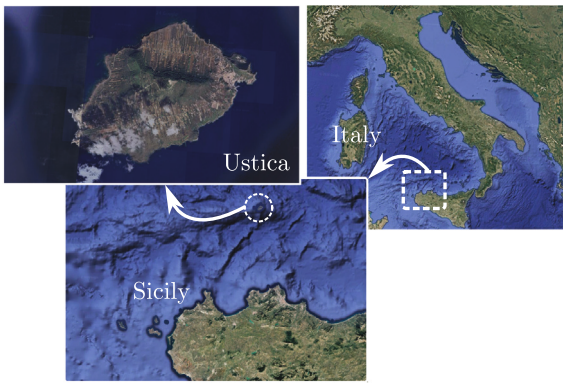


**Fig. 10.** Geographical location of the island of Ustica.

As previously discussed, given the early stage of the analysed technology design, this study does not directly tackle CoE optimisation but instead decouples annual productivity information from cost expenditure. Therefore, the work in this paper aims to maximise the energy produced annually by the device (AEP, first objective function) while at the same time minimising its cost (CapEx, second objective function), thus defining a global multi-objective optimisation problem.

To solve the optimisation problem, the present study uses a Non-dominated Sorting Genetic Algorithm II (NSGA-II) [39]. The optimisation is implemented in MATLAB environment using the '*gamultiobj*' function. This framework is based on classic standard GA operators: selection, reproduction, crossover and mutation. The NSGA-II algorithm used also involves the introduction of controlled elitism in the solution with the aim of improving the variability in individuals and therefore the exploration of the design space in the process, and thus reducing the likelihood of the optimiser getting stuck in local minima.

Constraints, on the other hand, have been handled by means of penalty functions. Both geometrically unfeasible and hydrostatic unstable solutions are treated with penalty functions in order to direct the convergence towards feasible solutions. The parameters of individuals per generation ($N_{ind}$) and number of generations ($N_{gen}$) to be simulated were set to 70 and 150, respectively.

### 2.2. MILP energy planning model stage

The power system planning proposed in this study is based on a MILP problem developed within the PyPSA framework [69]. The objective of the MILP optimisation is to minimise the TAESC, which represents the $f_{obj}^{base}$ of the power system, as given in Eqs. (9)–(11), where $CC_{tot}$ and $OC_{tot}$ stand for the capital and operational costs, and $w(t)$ denotes the weight of each time step $t \in \Omega_T$.

The specific capital costs ($cc_{a,n}$) associated with each technology are multiplied by the corresponding installed capacity ($P_{a,n}$ for generation technologies or $E_{s,n}$ for battery energy storage systems, BESS). Similarly, the specific operational costs ($oc_{a,n}$) are multiplied by the electricity output of each technology ($d_{a,n,t}$), accounting for both the marginal fuel costs of conventional generators (e.g., diesel) and the variable operational costs of other technologies, such as degradation costs that depend on usage time.

$$\min f_{obj}^{base}, \text{ with } f_{obj}^{base} = CC_{tot} + OC_{tot} \tag{9}$$

$$CC_{tot} = \sum_{n\in\Omega_N} \left[ \sum_{a\in\Omega_R\cup\Omega_S} cc_{a,n} \cdot P_{a,n} + \sum_{s=1}^{\Omega_S} cc_{s,n} \cdot E_{s,n} \right] \tag{10}$$

$$OC_{tot} = \sum_{t\in\Omega_T} w_t \cdot \left( \sum_{n\in\Omega_N} \sum_{a\in\Omega_R\cup\Omega_S} oc_{a,n} \cdot d_{a,n,t} \right) \tag{11}$$

The electrical balance at each $n$th node in $\Omega_N$ is ensured by Eq. (12), where $f_{\ln,t}$ represents the power flow in the ln-th line, and $K_{\ln,n}$ is

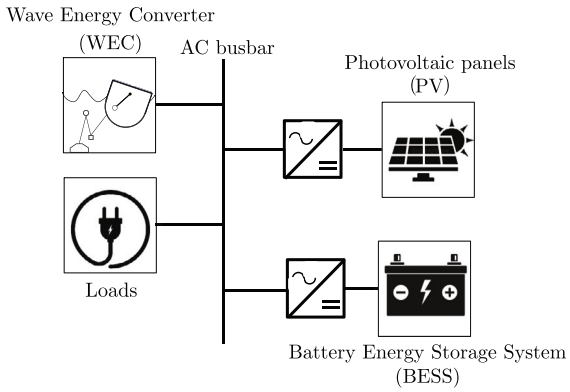


**Fig. 11.** Scheme of the adopted energy system.

the network's incidence matrix. This equation accounts for the interactions between power generation ($d_{a,n,t}$), storage discharging ($d^{dsc}_{s,n,t}$), and power flows, ensuring that they collectively satisfy the power demand ($l_{l,n,t}$) and storage charging ($d^{ch}_{s,n,t}$) at each node. The energy balance also considers the charge and discharge efficiencies of the storage system ($\eta^{ch}_{s,n}$ and $\eta^{dsc}_{s,n}$). Eqs. (13)–(14) impose operational constraints on the energy storage balance, where $e_{s,n,t}$ represents the state of charge of the $s$th storage system at the $n$th node at time $t$, and $E_{s,n}$ denotes the storage system's installed energy capacity, optimised as part of the model. Finally, Eq. (15) sets an upper limit on the renewable energy output, ensuring it does not exceed the available capacity. This constraint is defined by the capacity factor ($CF_{r,n,t}$) and the installed generation capacity ($P_{r,n}$).

$$\sum_{a\in(\Omega_G\cup\Omega_R)} d_{a,n,t} + \sum_{s\in\Omega_R} d^{dsc}_{s,n,t}\cdot\eta^{dsc}_{s,n} + \sum_{\ln\in\Omega_{LN}} f_{\ln,t}\cdot K_{\ln,n} = \sum_{s\in\Omega_R} \frac{d^{ch}_{s,n,t}}{\eta^{ch}_{s,n}} + \sum_{l\in\Omega_L} l_{l,n,t} \tag{12}$$

$$e_{s,n,t} = e_{s,n,t-1}\cdot(1-\eta^{ch}_{s,n}) - d^{dsc}_{s,n,t} + d^{ch}_{s,n,t}, \quad s\in\Omega_S \tag{13}$$

$$E_{s,n}\cdot e^{min}_{s,n,t} \le e_{s,n,t} \le E_{s,n}\cdot e^{max}_{s,n,t}, \quad s\in\Omega_S \tag{14}$$

**Table 3**
Cost assumptions.

| Technology | CapEx | OpEx | Op. Lifetime |
|---|---|---|---|
| PV | 905 ($\frac{€}{kW}$) | 17 ($\frac{€}{kW\cdot y}$) | 25 years |
| Li-ES | 300 ($\frac{€}{kWh}$) | 6 ($\frac{€}{kWh\cdot y}$) | 15 years |
| Power Converter | 180 ($\frac{€}{kW}$) | 180 ($\frac{€}{kW\cdot y}$) | 15 years |

$$0 \le d_{r,n,t} \le CF_{r,n,t}\cdot P_{r,n}, \quad r\in\Omega_R. \tag{15}$$

## 3. Case study: Ustica

The island of Ustica (Fig. 10), located in the southern Tyrrhenian Sea, approximately 53 km from the northern coast of Sicily, represents a unique case study for exploring local energy self-sufficiency through a microgrid energy planning model.

Ustica is a small, remote island of 8 km$^2$ with a stable population of 1300 inhabitants and a significant influx of tourists during the summer months. Currently, the island's electricity generation is mainly based on diesel generators, highlighting the urgent need for an energy transition to RES. The study investigates the feasibility of achieving 100% RES, focusing on lithium-ion energy storage (Li-ES), PV systems and WEC (see Fig. 11). In particular, the maximum PV capacity is limited to 4 MW due to spatial constraints, and onshore wind turbines are excluded due to local legal restrictions [70].

Given Ustica's abundant renewable resources but limited space for PV installations and the exclusion of onshore wind, the island is an ideal candidate for this analysis. The investment and operating costs associated with the selected RES technologies are summarised in Table 3, assuming a discount rate of 5% for financial evaluations [27,71].

In 2019, the island's annual electricity demand was approximately 4.9 GWh, with a peak load of 1.3 MW and a base load of 300 kW. Solar and wave energy resource hourly data (2019) were collected from the ERA5 platform [72]. The solar photovoltaic productivity have an average capacity factor of 19%, while detailed information on the wave energy resources can be found in Section 3.1. For the Li-ES system, based on [27], the following assumptions are made:

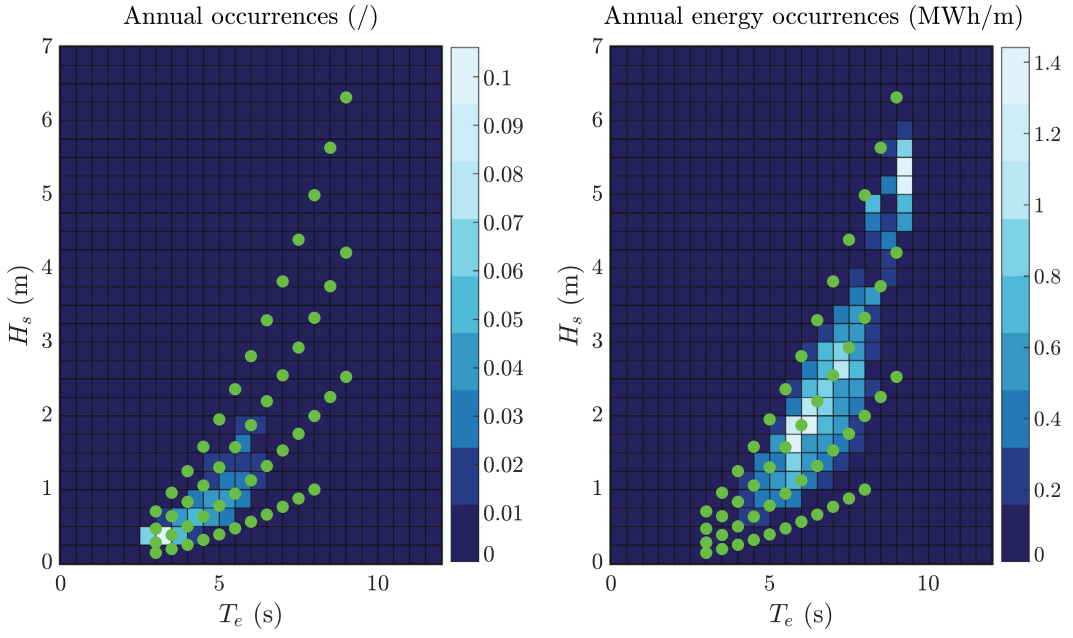


**Fig. 12.** Annual scatter diagrams for Ustica Island show annual occurrences (left) and annual energy density per metre of wave front (right). Green dots indicate the 50 representative waves selected for productivity estimation.

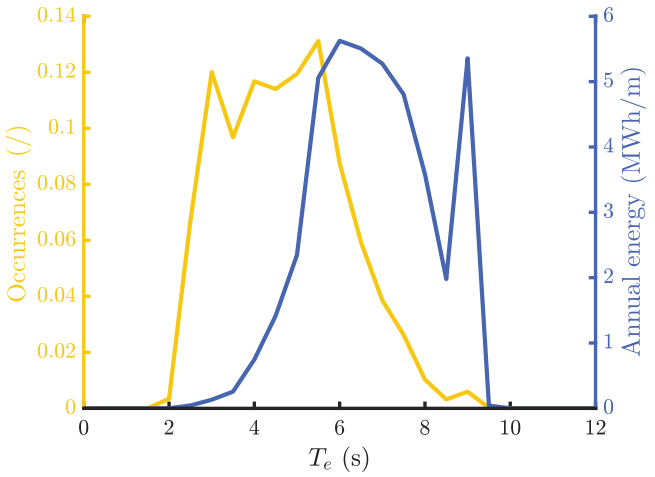


**Fig. 13.** Occurrences and energy density per metre of wave front distributions with respect to the energy period $T_e$. (For interpretation of the references to colour in this figure legend, the reader is referred to the web version of this article.)

- the round-trip efficiency equals to 90%, equally divided between charge and discharge;
- duration between 1 and 2 h;
- 30 €/MWh as degradation cost of Li-ES, obtained considering 10,000 lifetime cycles.

### 3.1. Ustica wave energy resource

Regarding the site under investigation in this work, the marine energy resource is represented in terms of its annual occurrences and its energy density per metre of wavefront.

These two parameters are represented by the scatter diagrams shown on the left and right of Fig. 12 with respect to the energy period $T_e$ and significant wave height $H_s$. The annual power density of the site is 4.8 kW/m.

In the same image, green markers are also reported, depicting the individual 50 sea states employed in the numerical model for the PTO control optimisation and the productivity assessment. Fig. 13 presents the distribution of wave occurrences and their energy in relation to the energy period $T_e$. The data indicate that most wave events occur around 4 s periods, whereas the most energetic waves are found near 6 s periods.

## 4. Results and discussion

The following section presents and discusses the results obtained by applying the procedure outlined in Section 2 to the previously described case study of the Ustica Island energy system.

### 4.1. Influence of power system integration on optimal device selection

The left image of Fig. 14 illustrates the solutions explored through the multi-objective optimisation, plotted as a function of the CapEx and AEP objective functions. Blue markers indicate the optimal devices that comprise the Pareto front. Notably, it is possible to individuate an area, with CapEx between 1.8 mln€ and 2.5 mln€, on which rely the most cost-effective WEC's design solutions in terms of CoE. The increase in CoE for both low and high CapEx derives from conversion inefficiencies and/or effects deriving from the boundaries of the search space set in the optimisation problem.

However, mapping the same results using a TAESC colourmap, as shown on the right plot of Fig. 14, reveals a different set of optimal design solutions for CapEx between 0.5 mln€ and 1.5 mln€.

Furthermore, the results show that some optimal devices belonging to the AEP-CapEx Pareto front exhibit suboptimal TAESC values, demonstrating that optimising system performance without information and integration of the energy system leads to the selection of suboptimal devices.

To assess the impact of energy system integration on selecting the optimal WEC device, Fig. 15 presents the remapping of solutions explored during optimisation based on the CoE and TAESC metrics. The results indicate that CoE and TAESC are conflicting objective functions, demonstrating that optimising a WEC device without accounting for its integration into the energy system leads to suboptimal device choices.

Furthermore, Figs. 16 and 17 detail the key design parameters of the devices and the system's techno-economic metrics for the optimal solutions on the CoE-TAESC Pareto front. This analysis provides deeper insight into how WEC integration influences system parameters. It is important to note that any significant discontinuities in the parameters may result from the CoE-TAESC Pareto front being derived through remapping rather than from an optimisation process specifically targeting these metrics.

In Fig. 16, a clear trend emerges where WECs optimised for higher TAESC (*i.e.* lower CoE) are characterised by larger hull length, greater displacement mass and pendulum mass. These choices result in resonance periods around 6 s, which correspond to high-energy (higher AEP) but less frequent wave conditions. In contrast, for lower TAESC devices exhibit shorter hulls, and smaller pendulum and displacement

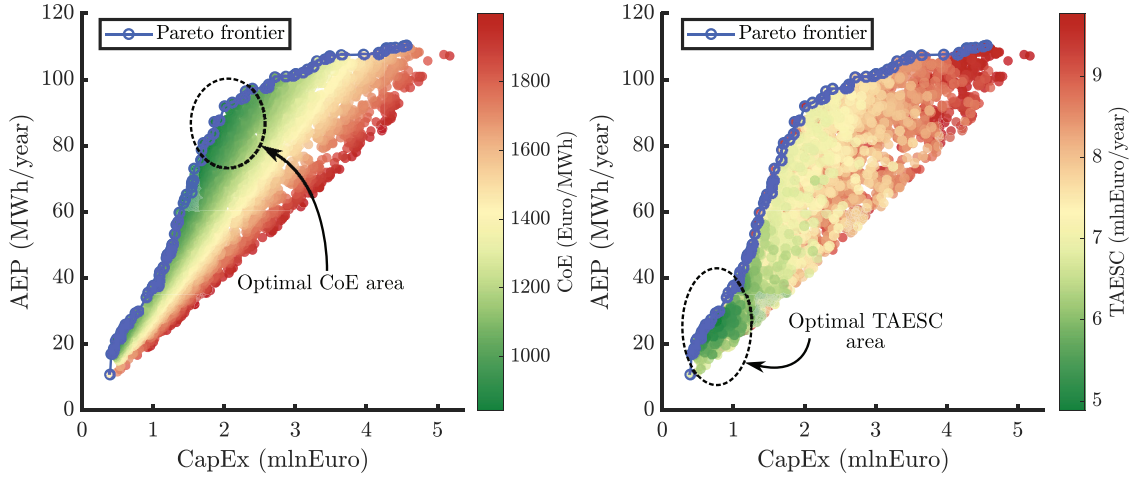


**Fig. 14.** GA optimisation outcomes. In blue the Pareto frontier. The colourmap illustrates the CoE (on the left) and TAESC (on the right) of the examined devices, highlighting both the optimal CoE and TAESC areas.

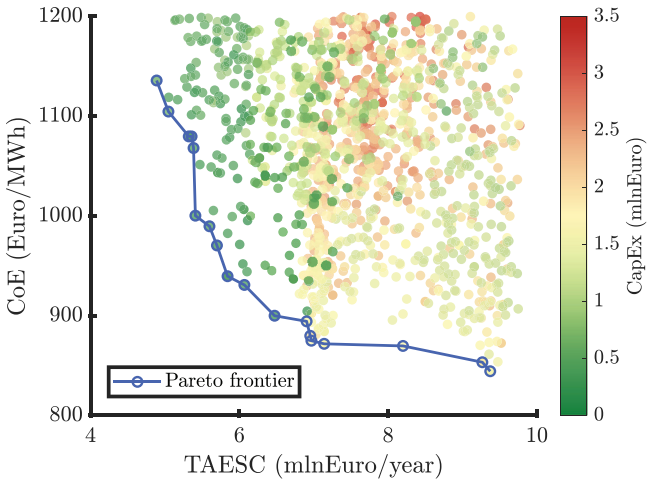


**Fig. 15.** GA optimisation outcomes remapped in the CoE-TAESC space with the colourmap illustrating the CapEx.

mass. This leads to resonance periods closer to 4.5 s, better matching the more frequently occurring, though less energetic, sea states at the Ustica site (see Fig. 13). Notably, the low TAESC design achieves similar annual operating hours despite a lower AEP, indicating better exploitation of wave energy. This behaviour directly influences energy production curtailment, as the energy system favours more continuous, albeit lower, energy generation over high-output production during limited time periods.

Fig. 17 shows how these design differences propagate to the system level. Devices that align with frequent sea states experience significantly lower curtailment, contributing to a lower TAESC. The total installed WEC capacity and associated CapEx are lower for the low TAESC case. The increased operational continuity of these WECs results in smoother and more predictable contributions to the energy mix, further enhancing system reliability and economic efficiency.

In energy systems with high RES penetration, the installed storage capacity (with its associated costs) is a key factor in order to ensure continuity of supply and in maintaining a proper grid balance of the energy system network. The amount of installed energy capacity of BESS ($E_{BESS}$) influences the need for energy imports while help to manage the critical excess production resulting by the natural variability of RES-generated electricity. Therefore, in order to analyse the effects of RES diversification into wave and PV within the Ustica's energy system, the correlation between $E_{BESS}$ and the installed capacity of wave energy ($P_{WEC}$) is mapped in Fig. 18.

Assuming that minimising storage capacity is optimal to reduce costs, the dispersion of points in the $P_{WEC}$-$E_{BESS}$ plane identifies an optimal range for the total installed WEC capacity between 0.5 MW and 2 MW.

Observing the colorbars in the left and right plots of the same Figure (representing TAESC and CoE respectively) it is noticed that the highest TAESC values are concentrated within the optimal WEC capacity range mentioned above. In contrast, the most efficient CoE configurations correspond to higher installed WEC capacities. Both the two regions are highlighted by black circles in the figure. The highlighted difference between CoE and TAESC optimality align with previous results, suggesting that the energy system tends to favour a more stable and continuous energy output, even if with lower power output, rather than a higher but more intermittent production.

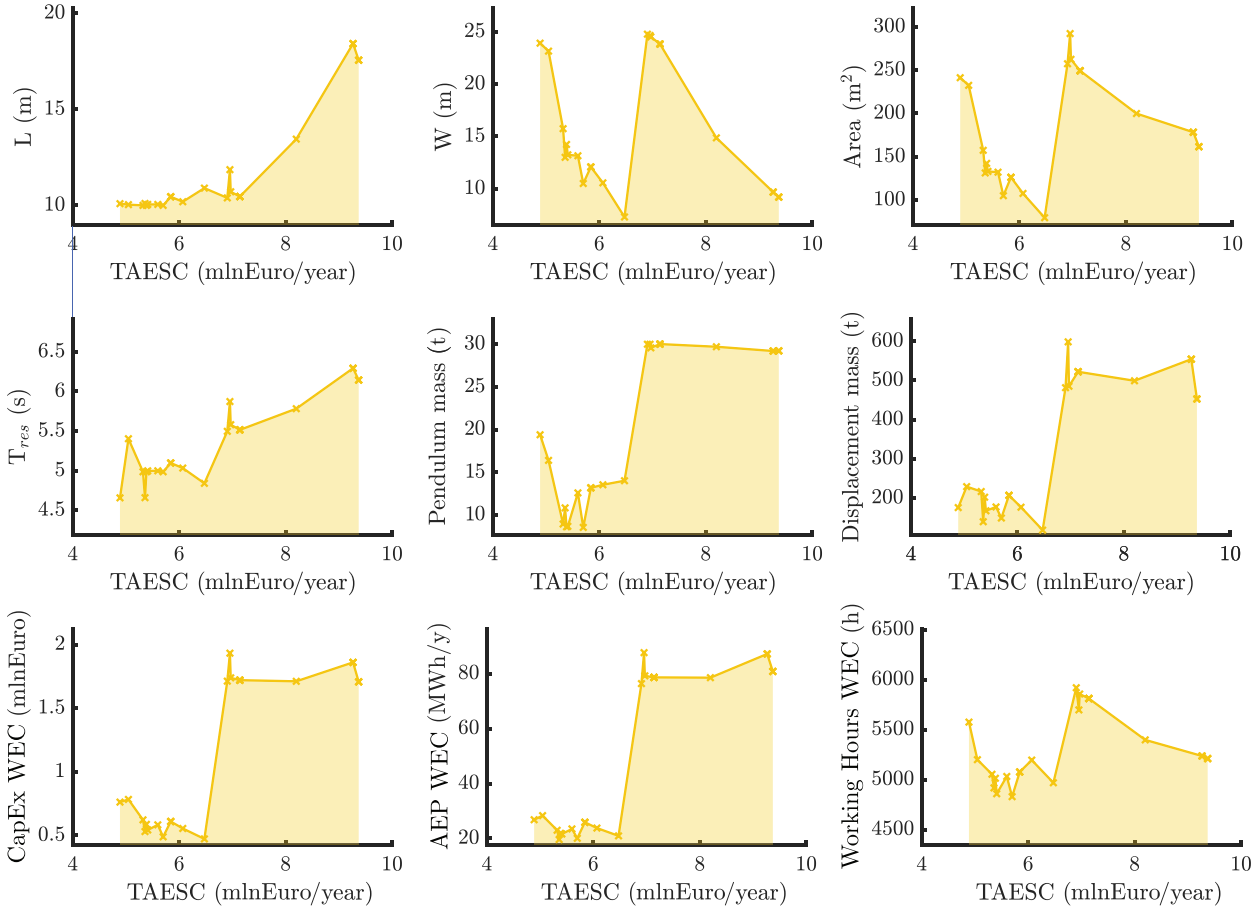


**Fig. 16.** Design parameters trends of device belonging to the CoE-TAESC Pareto's set.

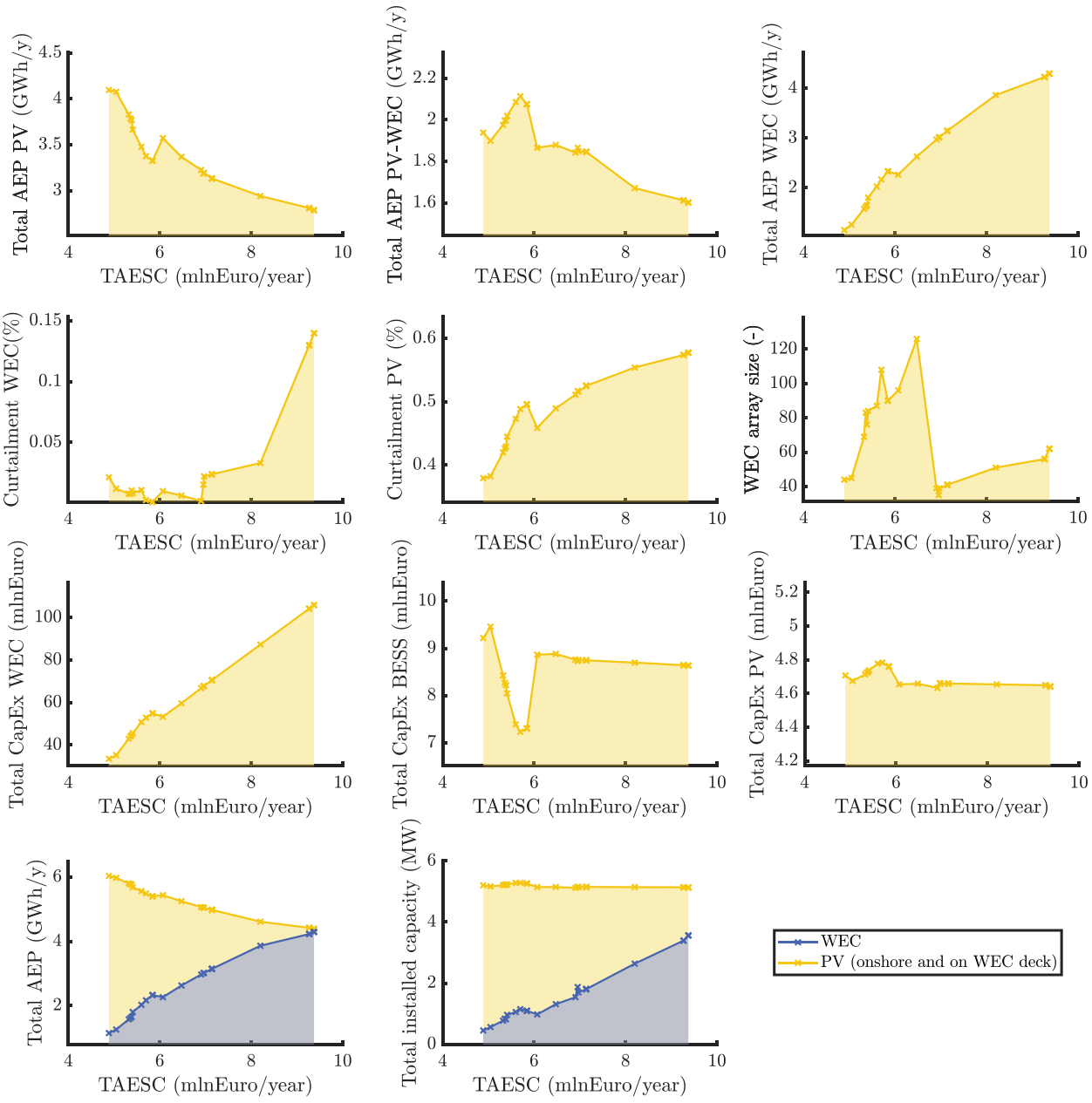


**Fig. 17.** Energy system parameters trends of device belonging to the CoE-TAESC Pareto's set.

### 4.2. Comparison of TAESC and CoE optimal devices

The analysis in this subsection move now towards the comparison of the two CoE and TAESC optimal extreme solutions among the all analysed WEC's design, with the aim to systematically highlight their differences and to provide a clear understanding of their distinct characteristics.

In order to provide a synthetic summary of the two WECs solutions analysed, Table 4 lists all their main design parameters and performances. As aspected considering the previously highlighted results, the CoE optimal WEC's design presents higher AEP (and concurrently also higher CapEx) than the TAESC optimal device but the previously suggested difference in continuity of operation can be also observed in different amount of annual working hours.

In addition, the geometrical dimensions of the hulls are depicted in frontal and top view plot of Fig. 19. The TAESC optimal device generally is designed as a smaller device compared to the CoE optimal solution, with around a 2.5 ratio both in terms of displacement volume

**Table 4**
Optimal devices design parameters.

| Parameter | Unit | CoE Optimal | TAESC Optimal |
|---|---|---|---|
| CapEx | (mln€) | 1.70 | 0.76 |
| AEP | (MWh/y) | 81.00 | 26.80 |
| Hull length | (m) | 17.5 | 10 |
| Hull width | (m) | 9.2 | 23.9 |
| Hull height | (m) | 8.51 | 3.78 |
| Hull draft | (m) | 4.43 | 1.43 |
| Pitch resonance period | (s) | 6.1 | 4.6 |
| Pendulum mass | (t) | 29.2 | 19.4 |
| Pendulum arm length | (m) | 2.0 | 1.0 |
| Displacement volume | ($m^3$) | 442 | 171 |
| Displacement mass | (t) | 453 | 175 |
| Working hours | (h) | 5083 | 5941 |
| Power installed capacity WEC | (kW) | 57.5 | 10.3 |
| PV installed capacity on deck | (kW) | 18.2 | 27.3 |

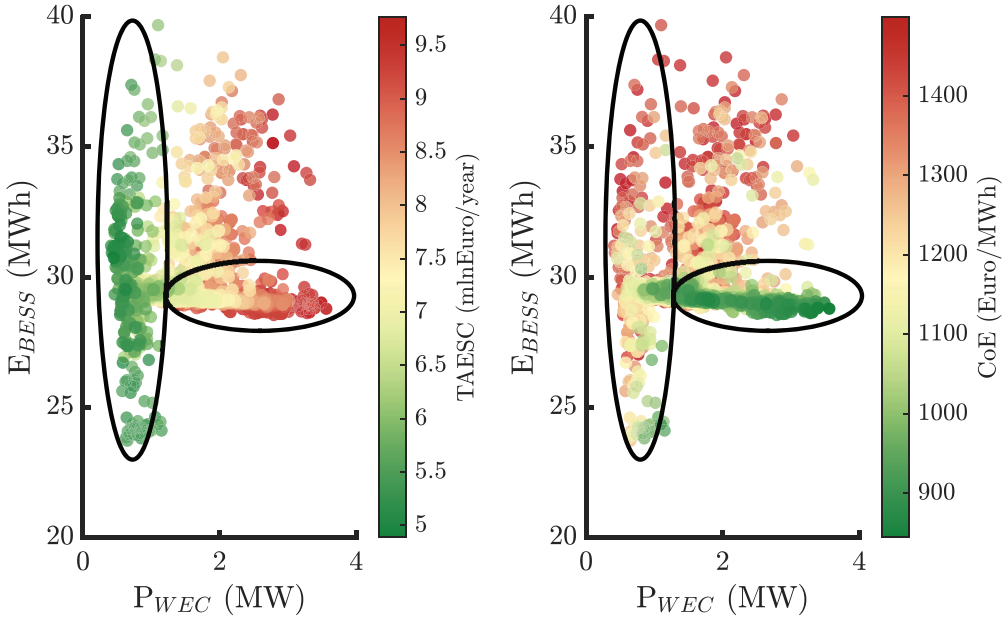


**Fig. 18.** Optimal nominal installed capacity of WECs ($P_{WEC}$) with respect to the energy capacity of the BESS ($E_{BESS}$). In black are highlighted the areas where the major differences have been found in terms of CoE and TAESC (in colourmaps) for the same set of individuals.

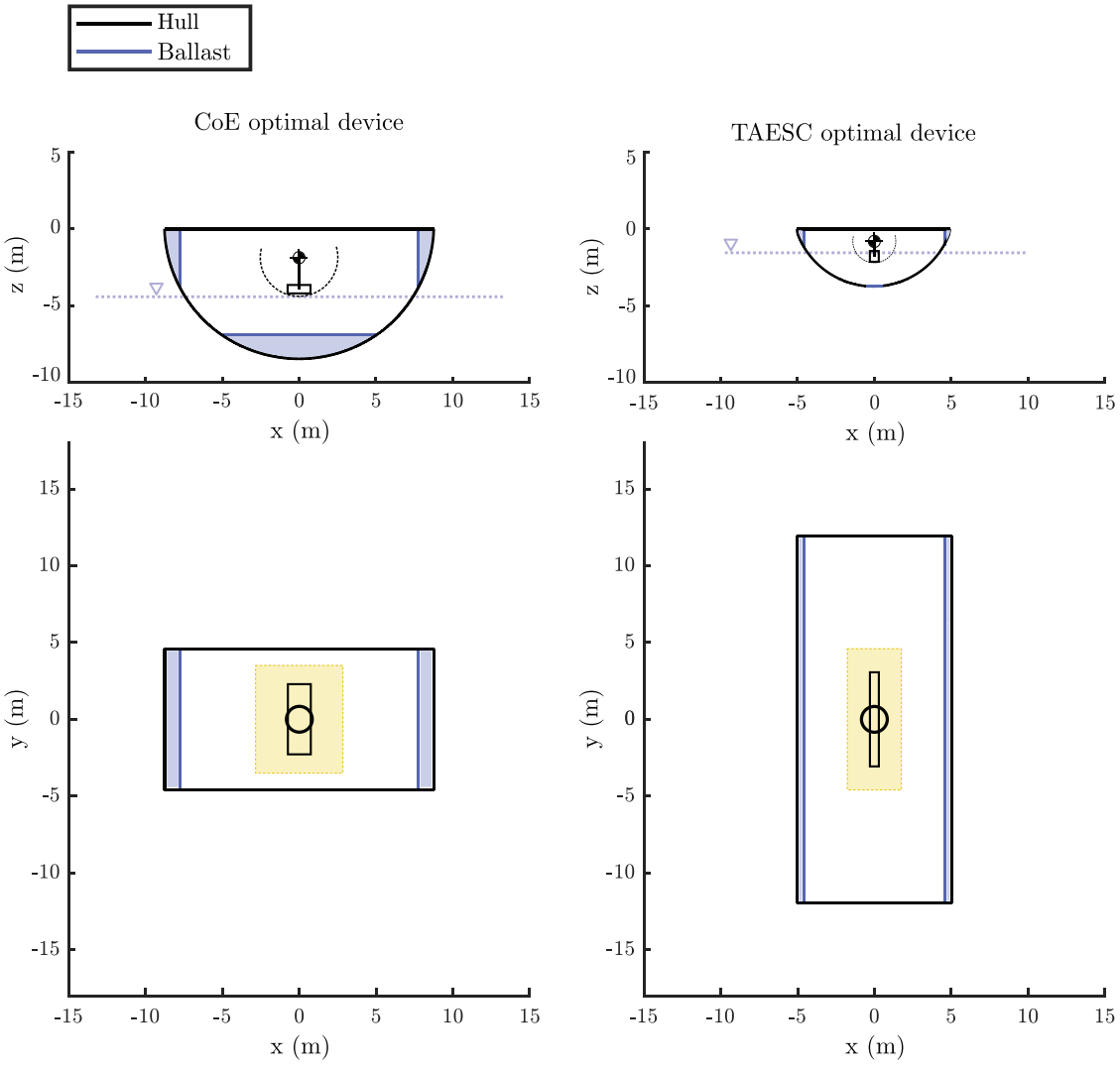


**Fig. 19.** Optimal devices comparison in dimensions. Frontal view in the upper part of the image and plant vision in the bottom line. In yellow is highlighted the pendulum unit area.

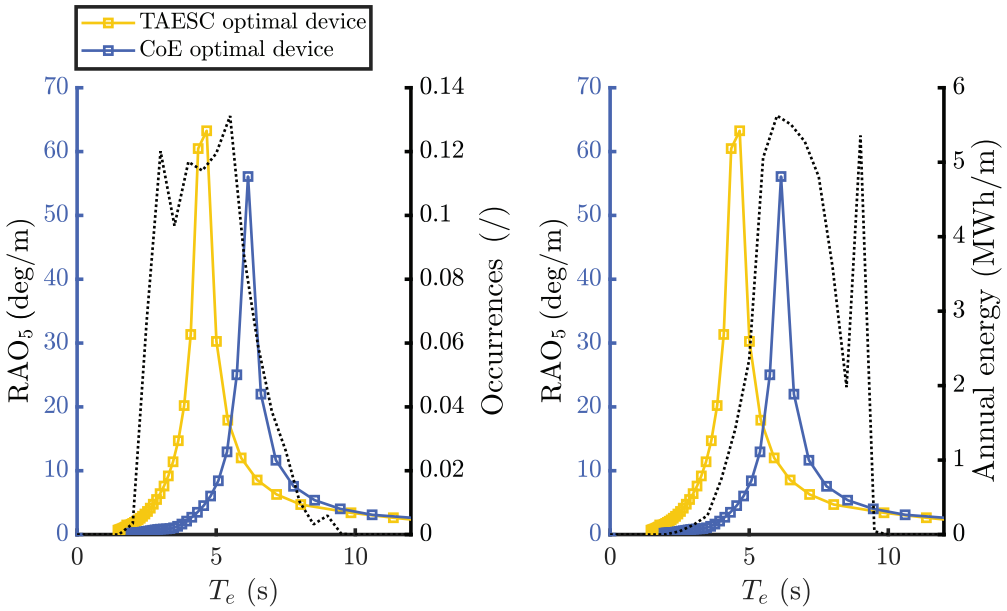


**Fig. 20.** Response amplitude operator on the pitch degree of freedom ($RAO_5$) over period for CoE (blue) and TAESC (yellow) optimal devices. The frequency responses are depicted in contrast with the resource's occurrences and energy density distributions (black dashed lines) over period. (For interpretation of the references to colour in this figure legend, the reader is referred to the web version of this article.)

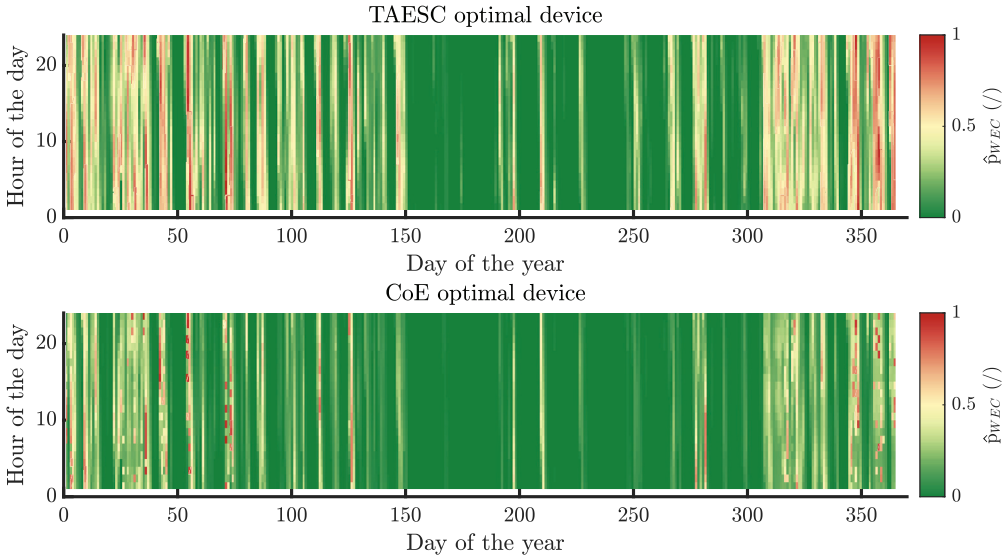


**Fig. 21.** Normalised WEC's power production map. (For interpretation of the references to colour in this figure legend, the reader is referred to the web version of this article.)

and mass. Looking to the hull dimension, CoE optimal WEC is bigger both considering the overall device height and length, but shorter along the *y*-axis dimension compared to the TAESC optimal solution.

Furthermore, the frequency responses to wave external forces according to the pitch degree of freedom (*i.e.* the Response Amplitude Operator, RAO) of the devices are shown in Fig. 20. Given that for the PeWEC the optimal operating condition is the one for which we come as close as possible to the resonance of the system, since more oscillations correspond to higher WEC productivity, what is noticed in the calculated RAOs is consistent with what has been achieved by previous outcomes of the present study. The CoE optimal device exhibits the characteristic peak of the resonance condition of a second-order system for periods of about 6 s, which can be attested to the most energetic marine conditions. In contrast, the resonance conditions of the TAESC optimal device are found at lower periods, corresponding to a range of lower energetic but most recurrent sea states.

By overlaying the two RAO responses with the annual occurrences and energy density spectra, it emerges that the TAESC optimal device is matched by the peak number of occurrences while the CoE optimal WEC frequency behaviour is matched by the period of maximum energy density per wave metre over the course of the year. This trend is consistent with the behaviours highlighted above, *i.e.* the device capable of minimising the annual energy system cost corresponds to greater continuity in terms of operation (aling its optimal operative condition with the greater number of occurrences) while the WEC that minimises the CoE match its RAO's peak with a period similar to the annual peak energy period. Consistent with the research conducted in [73] and [74], the outcomes show that the economic viability of a WECs is linked to optimal designs that target sea states characterised by lower $T_e$ (albeit with a lower wavefront energy density) but much more occurrent than highly energetic sea states (great $H_s$ and $T_e$).

Delving into the whole energy system techno-economic perspective, Fig. 21 shows the annual maps of the electrical power ($p_{WEC}$) produced

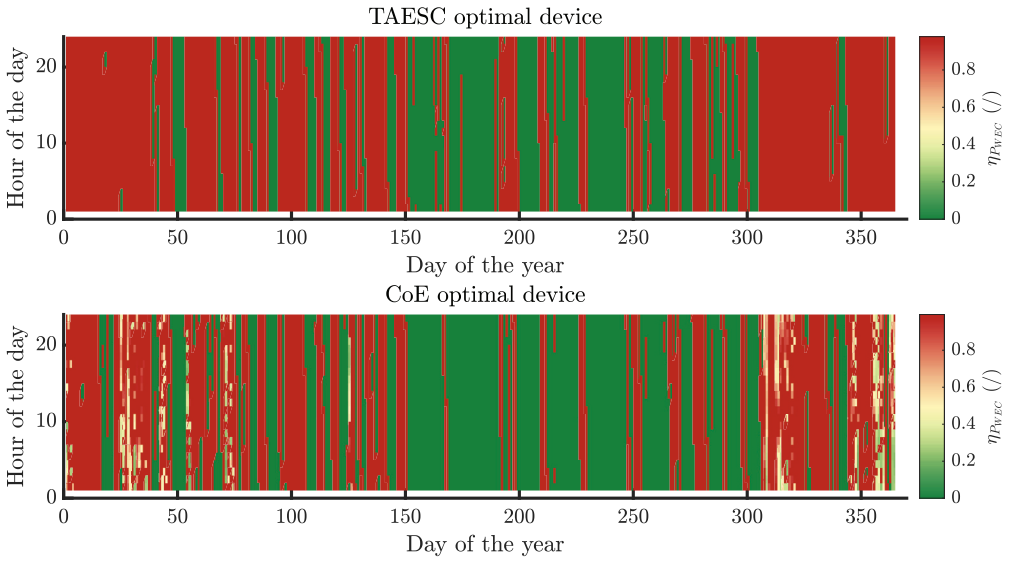


**Fig. 22.** Optimal WECs' conversion efficiency. (For interpretation of the references to colour in this figure legend, the reader is referred to the web version of this article.)

by each of the two devices during the year under investigation. The maps are shaped as cell-grid created by intersecting the days of the year (x-axis) with the hours of the day (y-axis) and colouring each of each cell according to the magnitude of the variable under consideration. In Fig. 21, as anticipated, the power produced over time by the two investigated devices is illustrated, but since these devices have different power sizes, the WEC power has been normalised ($\hat{p}_{WEC}$) with respect to the maximum annual value of WEC's power ($p^{max}_{WEC}$) in order to enable the two systems to be comparable (Eq. (16)):

$$\hat{p}_{WEC} = \frac{p_{WEC}}{p^{max}_{WEC}} \tag{16}$$

The utilisation characteristics of the two systems differ since the TAESC optimal device exhibits a much more continuous and occurring power output over the course of days than the corresponding CoE optimal device. In fact, many more yellow and red areas can be seen in the map compared to the CoE optimal device's one, where green is much more present along with red peaks in some sparse cells.

Similarly, the grid map of Fig. 22 shows a disparity in the capacity of the device to produce power compared to the theoretically producible power. This information on the performance of the WEC is provided by $\eta_{p_{WEC}}$, which the formulation of which is described by Eq. (17):

$$\eta_{p_{WEC}} = \frac{p_{WEC}}{p_{0,WEC}} \tag{17}$$

where $p_{0,WEC}$ is the maximum theoretically producible power in that hour, defined as the power that could be generated by the WEC assuming no curtailment is required for system balancing (*e.g.*, due to low demand or restricted BESS capacity). Again, the CoE optimal device has a lower and less continuous performance, denoted in the graph by the yellow spots (*i.e.* lower $\eta_{p_{WEC}}$) where for the corresponding TAESC optimal device, red is predominant.

Table 5 reports a complete overview of the techno-economic data of the two achieved scenarios for the Ustica's energy system.

Due to the higher efficiency in harnessing marine energy potential (as indicated by curtailment values) and the nearly identical total installed PV capacity (both onshore and on WEC decks), the TAESC optimal scenario requires a smaller WEC array size. A minor number of installed WECs leads to cost savings in both initial investment (CapEx) and the annualised costs of the three main subsystems, *i.e.* BESS, PV, and WEC. The utilisation of the optimal TAESC design results in an annual saving of 4.49 mln€/y, representing a 47.9% reduction in costs, despite a lower total AEP from wave energy.

**Table 5**
Optimal devices energy systems parameters and performance indicators. In the table, *CF* stands for the mean Capacity Factor, evaluated as the ratio between the mean power produced along the year over the total installed capacity.

| Parameter | Unit | CoE Optimal | TAESC Optimal |
|---|---|---|---|
| CoE | (€/MWh) | 844 | 1135 |
| TAESC | (mln€/y) | 9.37 | 4.88 |
| WEC array size | (/) | 62 | 44 |
| Total capacity of WEC | (MW) | 3.56 | 0.45 |
| Total capacity of PV | (MW) | 4 | 4 |
| Total capacity of PV-WEC | (MW) | 1.12 | 1.20 |
| Total capacity of BESS | (MW) | 14.40 | 15.40 |
| Total AEP WEC | (GWh/y) | 4.20 | 1.14 |
| Total AEP PV | (GWh/y) | 2.80 | 4.09 |
| Total AEP PV-WEC | (GWh/y) | 1.60 | 1.90 |
| *CF* WEC | (/) | 0.07 | 0.14 |
| *CF* PV | (/) | 0.10 | 0.13 |
| Curtailment WEC | (/) | 0.14 | 0.02 |
| Curtailment PV | (/) | 0.48 | 0.30 |
| WEC annual cost | (mln€/y) | 6.77 | 2.15 |
| PV annual cost | (mln€/y) | 0.70 | 0.70 |
| BESS annual cost | (mln€/y) | 1.90 | 2.03 |

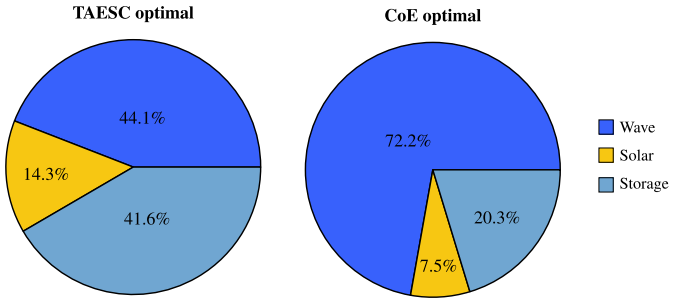


**Fig. 23.** Annual costs breakdown for TAESC and CoE optimal WEC designs.

The percentage breakdown of the energy system costs for both scenarios is shown in Fig. 23. The pie charts illustrate that the increase in TAESC is proportional to the share of annual costs associated with wave energy. Despite a higher energy cost than the CoE efficient WEC, the TAESC optimal WEC design is able to better exploit wave energy by improving its real value. In the studied case, by the share of annual costs covered by wave energy is reduced from 72.2% to 44.1%, which is comparable to the annual cost share of storage.

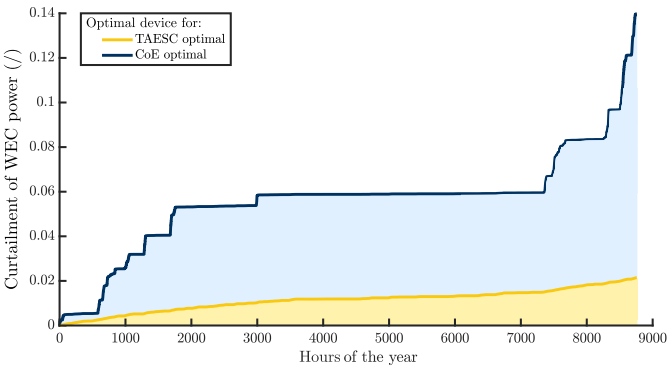


**Fig. 24.** Optimal devices power curtailment: in yellow for the TAESC optimal device and in blue for the CoE optimal WEC. (For interpretation of the references to colour in this figure legend, the reader is referred to the web version of this article.)

Consistently, Fig. 24 shows the cumulative graph over time of unexploited power ($p_{0,WEC} - p_{WEC}$) over the total producible power ($p^{tot}_{0,WEC}$), *i.e.* curtailment in Eq. (18):

$$\text{Curtailment} = \frac{p_{0,WEC} - p_{WEC}}{p^{tot}_{0,WEC}} \tag{18}$$

The chart clearly shows that the CoE optimal device exhibits a significantly higher amount of untapped power compared to the TAESC optimal device. In fact, this is noticeable because the curtailment of the CoE optimal WEC is always at a higher value than those of the second device, and at the end of the year, the total unexploited power loss amounts to 14% for the first WEC compared to 2% for the second.

To assess the robustness of the key findings (namely, that power consistency has a greater impact on overall system costs than AEP) a sensitivity analysis was conducted on the two WEC devices identified as optimal under the TAESC and CoE criteria. This analysis evaluates how variations in cost assumptions affect the relative change in TAESC (ΔTAESC). Specifically, we examined the effect of ±30% perturbations in the costs of the three primary system components: WECs, PV, and BESS.

Fig. 25 illustrates the sensitivity of the TAESC and CoE optimal designs, showing the relative change in TAESC (ΔTAESC, in %) as a function of cost multipliers for each subsystem. Solid lines represent the TAESC-optimal device, while dotted lines correspond to the CoE optimal device. The nominal case (*i.e.*, multiplier equals to 1) is indicated by the dashed horizontal line. The TAESC optimal design consistently demonstrates lower sensitivity to variations in WEC and PV costs compared to the CoE optimal design. In contrast, it shows slightly higher sensitivity to BESS cost variations, despite only a 1 MW difference in installed storage capacity. Overall, the results indicate that both systems' TAESC is most sensitive to wave energy costs, followed by storage, and least sensitive to PV costs.

To further evaluate the resilience of the two optimal designs under broader uncertainty, a probabilistic analysis was conducted. Using a Monte Carlo approach with 5000 uniformly distributed samples representing cost variations across the three subsystems, we computed the probability density function of ΔTAESC for both devices. In Fig. 26, the yellow line represents the TAESC optimal design and the blue line the CoE optimal design. The TAESC optimal configuration displays a narrower distribution centred around zero, indicating superior robustness and stability with respect to the uncertain cost conditions.

Concerning the two scenarios analysed, and considering that the TAESC of the CoE optimal system would need to be reduced by approximately 48% to match that of the TAESC optimal solution, the results confirm that the design optimised for system-level performance are substantially more resilient to cost uncertainty.

## 5. Conclusions and further works

The techno-economic optimisation of WECs design is a widely studied topic in literature. The LCoE is a well-established metric for assessing techno-economic performance. However, due to the complexity and uncertainty inherent in WECs system models, as well as the early stage of such technology, it may not always be the most suitable metric. Additionally, LCoE does not account for the actual integration of WECs within a broader energy system.

In the present work, the PeWEC design has been optimised via a GA-based multi-objective framework that aims to simultaneously minimise the WEC's CapEx and maximise its AEP. Each optimised design solution is then integrated into a system-wide energy model, followed by a second optimisation round. This phase, conducted via PyPSA, focuses on minimising the TAESC of the Ustica energy system.

The proposed framework enables a comprehensive evaluation of each design solution's performance within the power system. Moreover,

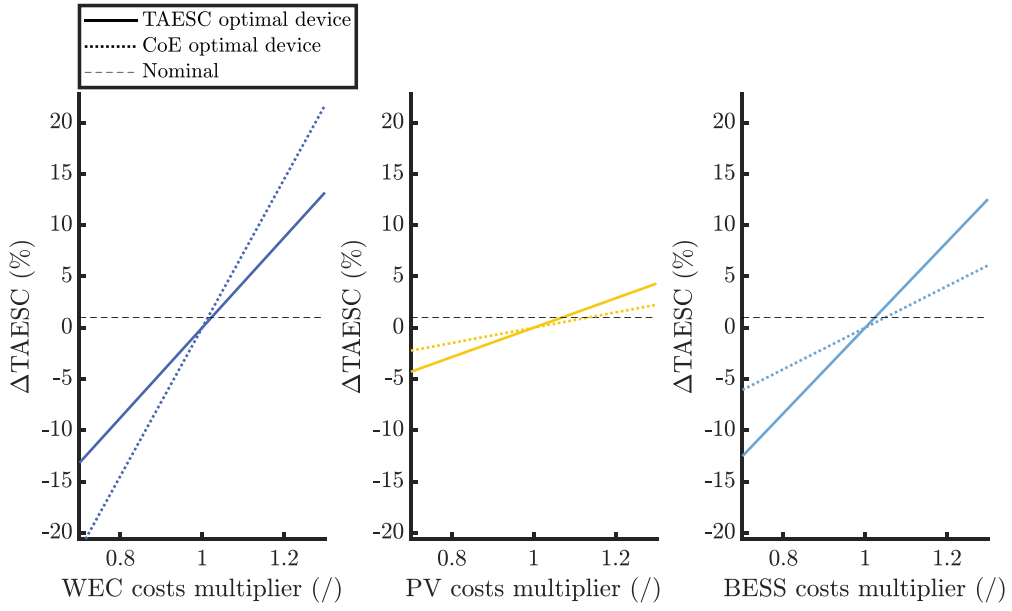


**Fig. 25.** Relative change in TAESC (ΔTAESC, in %) as a function of cost multipliers for WEC (left), PV (centre), and BESS (right).

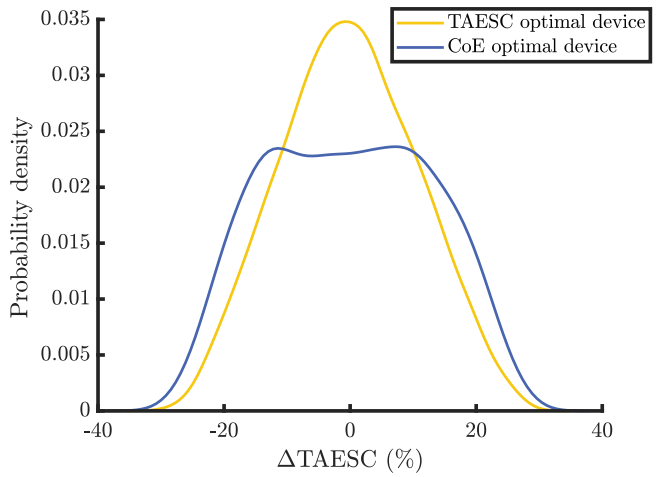


**Fig. 26.** Probability density function of the relative change in TAESC (ΔTAESC, in %) under stochastic cost scenarios. (For interpretation of the references to colour in this figure legend, the reader is referred to the web version of this article.)

the framework assesses the impact of WEC's design parameters on the system through a newly obtained CoE-TAESC map, ultimately leading to an updated Pareto frontier.

This study demonstrates that optimising WEC solely for cost minimisation leads to suboptimal choices when considering system-wide energy costs.

The device with the lowest CoE achieves an AEP of 81 MWh but requires a capital expenditure of 1.70 mln€, while the configuration minimising the TAESC generates only 26.8 MWh yet reduces CapEx to 0.76 mln€. Despite lower energy production, the TAESC optimal design leads to a 47.9% reduction in total annual system costs, primarily due to higher operational continuity (5941 hours/year vs. 5083) and a 7-fold reduction in curtailed energy (2% vs. 14%). The results indicate that economic viability is not dictated by cost per unit of energy alone but by how production aligns with system demand and the availability of other renewable sources.

A key finding is that optimising for system-wide costs inherently prioritises devices that generate energy more consistently across the year, rather than those maximising production during high-energy but infrequent wave events. This shifts the economic justification for wave energy technologies from cost competitiveness alone towards their value of energy, defined by their ability to generate electricity when solar and wind resources are insufficient. The system-level analysis shows that a device designed for lower total system costs results in a more effective integration into the grid, and a better balance between production and consumption.

These results highlight the need to redefine optimisation metrics for emerging offshore renewable technologies. Rather than minimising energy costs in isolation, system-level models should incorporate the value of energy as a core objective. By designing wave energy converters to complement vRES rather than simply maximising output, they can improve their integration into energy systems, and enhance overall cost efficiency.

In conclusion, the present analysis suggests the likelihood necessity to incorporate the power grid information directly into the optimisation process, *i.e.* developing a power-grid informed optimisation. A proper grid-informed WEC design optimisation would enable the designer to investigate the actual advantage of wave energy production integration into a energy system.

### 5.1. Limitations and future work

While the proposed methodology provides a novel and integrated framework for WEC design and energy system co-optimisation, several limitations should be acknowledged. First, the analysis focuses on a single case study (PeWEC as WEC and Ustica Island as site), and although the methodology is generalisable, site-specific insights may vary in different contexts. Second, the current optimisation framework does not incorporate a formal treatment of uncertainty. Although a sensitivity and probabilistic analysis was performed on the main cost parameters, a more rigorous robust optimisation process, accounting for cost uncertainty and systemic interactions, would be more appropriate for guiding decision-making under uncertainty. Addressing these limitations represents a key objective for future work, including the implementation of stochastic and adaptive optimisation frameworks as well as multi-location validation. Moreover, future research should refine these models by including dynamic market conditions, pricing mechanisms, and a broader range of operational constraints, ensuring that offshore renewable technologies are evaluated within the full complexity of power system planning.

## CRediT authorship contribution statement

**Filippo Giorcelli:** Writing – review & editing, Methodology, Data curation, Software, Formal analysis, Writing – original draft, Investigation, Conceptualization. **Enrico Giglio:** Software, Formal analysis, Writing – original draft, Investigation, Conceptualization, Writing – review & editing, Methodology, Data curation. **Sergej Antonello Sirigu:** Validation, Resources, Investigation, Conceptualization, Writing – review & editing, Software, Methodology, Formal analysis, Supervision, Project administration, Funding acquisition. **Giuliana Mattiazzo:** Project administration, Supervision, Writing – review & editing, Funding acquisition.

## Declaration of competing interest

Filippo Giorcelli reports financial support was provided by ENI. Giuliana Mattiazzo reports financial support was provided by Ministry of Education and Merit. If there are other authors, they declare that they have no known competing financial interests or personal relationships that could have appeared to influence the work reported in this paper.

## Acknowledgements & Funding

The authors express their gratitude for the funds received from the Ministry of University and Research and PNRR's PhD scholarship program defined in DM-352/2022 in collaboration with Eni S.p.A. This publication is part of the PNRR-NGEU project.

Moreover, the Project is funded under the National Recovery and Resilience Plan (NRRP), Italy, Mission 4 Component 2 Investment 1.3 - Call for tender No. 1561 of 11.10.2022 of Ministero dell' Università e della Ricerca (MUR); funded by the European Union – NextGenerationEU Award Number: Project code PE0000021, Concession Decree No. 1561 of 11.10.2022 adopted by Ministero dell'Università e della Ricerca (MUR), Italy, CUP, Italy E13C22001890001, Project title "Network 4 Energy Sustainable Transition – NEST

## Data availability

Data will be made available on request.

## References

[1] IRENA. 100% renewable energy scenarios: Supporting ambitious policy targets. 2024, URL https://www.irena.org/Publications/2024/Mar/100pc-renewable-energy-scenarios-Supporting-ambitious-policy-targets. [Accessed 27 March 2025].

[2] Connolly D, Lund H, Mathiesen BV, Leahy M. A review of computer tools for analysing the integration of renewable energy into various energy systems. Appl Energy 2010;87(4):1059–82.

[3] Giglio E, Luzzani G, Terranova V, Trivigno G, Niccolai A, Grimaccia F. An efficient artificial intelligence energy management system for urban building integrating photovoltaic and storage. IEEE Access 2023;11:18673–88.

[4] Giglio E, Fioriti D, Chihota MJ, Poli D, Bekker B, Mattiazzo G. Integrated stochastic reserve estimation and MILP energy planning for high renewable penetration: Application to 2050 South African energy system. Sustain Energy Grids Netw 2025;42:101650.

[5] Colmenar-Santos A, Linares-Mena A-R, Molina-Ibáñez E-L, Rosales-Asensio E, Borge-Diez D. Technical challenges for the optimum penetration of grid-connected photovoltaic systems: Spain as a case study. Renew Energy 2020;145:2296–305.

[6] Rosales-Asensio E, Diez DB, Sarmento P. Electricity balancing challenges for markets with high variable renewable generation. Renew Sustain Energy Rev 2024;189:113918.

[7] Quitoras MR, Cabrera P, Campana PE, Rowley P, Crawford C. Towards robust investment decisions and policies in integrated energy systems planning: Evaluating trade-offs and risk hedging strategies for remote communities. Energy Convers Manage 2021;229:113748.

[8] Marocco P, Ferrero D, Lanzini A, Santarelli M. The role of hydrogen in the optimal design of off-grid hybrid renewable energy systems. J Energy Storage 2022;46:103893.

[9] Fusco F, Nolan G, Ringwood JV. Variability reduction through optimal combination of wind/wave resources–An Irish case study. Energy 2010;35(1):314–25.

[10] Pérez-Collazo C, Greaves D, Iglesias G. A review of combined wave and offshore wind energy. Renew Sustain Energy Rev 2015;42:141–53.

[11] Guo B, Ringwood JV. A review of wave energy technology from a research and commercial perspective. IET Renew Power Gener 2021;15(14):3065–90.

[12] Guo B, Ringwood JV. Geometric optimisation of wave energy conversion devices: A survey. Appl Energy 2021;297:117100.

[13] Garcia-Teruel A, Forehand D. A review of geometry optimisation of wave energy converters. Renew Sustain Energy Rev 2021;139:110593.

[14] Trueworthy A, DuPont B. The wave energy converter design process: Methods applied in industry and shortcomings of current practices. J Mar Sci Eng 2020;8(11):932.

[15] Clark CE, Teruel AG, DuPont B, Forehand DI. Towards reliability-based geometry optimization of a point-absorber with PTO reliability objectives. In: 13th European wave and tidal energy conference. 2019.

[16] Cordonnier J, Gorintin F, De Cagny A, Clément A, Babarit A. SEAREV: Case study of the development of a wave energy converter. Renew Energy 2015;80:40–52.

[17] Teillant B, Costello R, Weber J, Ringwood J. Productivity and economic assessment of wave energy projects through operational simulations. Renew Energy 2012;48:220–30.

[18] Portillo J, Reis P, Henriques J, Gato L, Falcão A. Backward bent-duct buoy or frontward bent-duct buoy? Review, assessment and optimisation. Renew Sustain Energy Rev 2019;112:353–68.

[19] Sirigu SA, Foglietta L, Giorgi G, Bonfanti M, Cervelli G, Bracco G, et al. Techno-economic optimisation for a wave energy converter via genetic algorithm. J Mar Sci Eng 2020;8(7):482.

[20] Giglio E, Petracca E, Paduano B, Moscoloni C, Giorgi G, Sirigu SA. Estimating the cost of wave energy converters at an early design stage: A bottom-up approach. Sustainability 2023;15(8):6756.

[21] Garcia-Teruel A, Forehand DI. Manufacturability considerations in design optimisation of wave energy converters. Renew Energy 2022;187:857–73.

[22] Garcia-Teruel A, Clark CE. Reliability-based hull geometry optimisation of a point-absorber wave energy converter with power take-off structural reliability objectives. IET Renew Power Gener 2021;15(14):3255–68.

[23] Clark CE, DuPont B. Reliability-based design optimization in offshore renewable energy systems. Renew Sustain Energy Rev 2018;97:390–400.

[24] Golbaz D, Asadi R, Amini E, Mehdipour H, Nasiri M, Etaati B, et al. Layout and design optimization of ocean wave energy converters: A scoping review of state-of-the-art canonical, hybrid, cooperative, and combinatorial optimization methods. Energy Rep 2022;8:15446–79.

[25] Coe RG, Ahn S, Neary VS, Kobos PH, Bacelli G. Maybe less is more: Considering capacity factor, saturation, variability, and filtering effects of wave energy devices. Appl Energy 2021;291:116763. http://dx.doi.org/10.1016/j.apenergy.2021.116763, URL https://www.sciencedirect.com/science/article/pii/S0306261921002701.

[26] Roventus S, Widodo S, Jonhariono S. Ocean potential: Strategies for integrating tidal and wave energy into national power grids. GEMOY: Green Energy Manag Optim Yields 2024;1(1):49–65, URL https://pubcenter.ristek.or.id/index.php/Gemoy/article/view/38.

[27] Giglio E, Novo R, Mattiazzo G, Fioriti D. Reserve provision in the optimal planning of off-grid power systems: Impact of storage and renewable energy. IEEE Access 2023;11:100781–97. http://dx.doi.org/10.1109/ACCESS.2023.3313979.

[28] Deng X, Lv T. Power system planning with increasing variable renewable energy: A review of optimization models. J Clean Prod 2020;246:118962. http://dx.doi.org/10.1016/j.jclepro.2019.118962, URL https://www.sciencedirect.com/science/article/pii/S0959652619338326.

[29] Novo R, Minuto FD, Bracco G, Mattiazzo G, Borchiellini R, Lanzini A. Supporting decarbonization strategies of local energy systems by de-risking investments in renewables: A case study on pantelleria Island. Energies 2022;15(3). http://dx.doi.org/10.3390/en15031103, URL https://www.mdpi.com/1996-1073/15/3/1103.

[30] Kluger JM, Haji MN, Slocum AH. The power balancing benefits of wave energy converters in offshore wind-wave farms with energy storage. Appl Energy 2023;331:120389. http://dx.doi.org/10.1016/j.apenergy.2022.120389, URL https://www.sciencedirect.com/science/article/pii/S0306261922016464.

[31] Said HA, Ringwood JV. Grid integration aspects of wave energy—Overview and perspectives. IET Renew Power Gener 2021;15(14):3045–64. http://dx.doi.org/10.1049/rpg2.12179, arXiv:https://ietresearch.onlinelibrary.wiley.com/doi/pdf/10.1049/rpg2.12179. URL https://ietresearch.onlinelibrary.wiley.com/doi/abs/10.1049/rpg2.12179.

[32] McCabe R, Dietrich M, Liu A, Haji M. System level techno-economic and environmental design optimization for ocean wave energy. In: International design engineering technical conferences and computers and information in engineering conference, Vol. 87301. American Society of Mechanical Engineers; 2023, V03AT03A033.

[33] Mai T, Mowers M, Eurek K. Competitiveness metrics for electricity system technologies. Tech. rep., National Renewable Energy Lab.(NREL), Golden, CO (United States); 2021.

[34] IRENA. Renewable power generation costs in 2019. 2020, URL https://www.irena.org/publications/2020/Jun/Renewable-Power-Costs-in-2019. [Accessed 15 May 2025].

[35] de Faria VA, de Queiroz AR, DeCarolis JF. Optimizing offshore renewable portfolios under resource variability. Appl Energy 2022;326:120012.

[36] Coe RG, Lavidas G, Bacelli G, Kobos PH, Neary VS. Minimizing cost in a 100% renewable electricity grid: A case study of wave energy in California. In: International conference on offshore mechanics and arctic engineering, Vol. 85932. American Society of Mechanical Engineers; 2022, V008T09A073.

[37] Coles D, Wray B, Stevens R, Crawford S, Pennock S, Miles J. Impacts of tidal stream power on energy system security: An isle of wight case study. Appl Energy 2023;334:120686. http://dx.doi.org/10.1016/j.apenergy.2023.120686, URL https://www.sciencedirect.com/science/article/pii/S0306261923000508.

[38] Blanco M, Navarro G, Najera J, Lafoz M, Sarasua JI, García H, et al. Wave farms integration in a 100% renewable isolated small power system -frequency stability and grid compliance analysis. Proc Eur Wave Tidal Energy Conf 2023;15. http://dx.doi.org/10.36688/ewtec-2023-215, URL https://submissions.ewtec.org/proc-ewtec/article/view/215.

[39] Deb K, Pratap A, Agarwal S, Meyarivan T. A fast and elitist multiobjective genetic algorithm: NSGA-II. IEEE Trans Evol Comput 2002;6(2):182–97.

[40] Carapellese F, Pasta E, Paduano B, Faedo N, Mattiazzo G. Intuitive LTI energy-maximising control for multi-degree of freedom wave energy converters: The PeWEC case. Ocean Eng 2022;256:111444.

[41] Dell'Edera O, Niosi F, Casalone P, Bonfanti M, Paduano B, Mattiazzo G. Understanding wave energy converters dynamics: High-fidelity modeling and validation of a moored floating body. Appl Energy 2024;376:124202.

[42] Paduano B, Carapellese F, Pasta E, Sirigu SA, Faedo N, Mattiazzo G. Data-based control synthesis and performance assessment for moored wave energy conversion systems: The PeWEC case. IEEE Trans Sustain Energy 2023;15(1):355–67.

[43] Niosi F, Begovic E, Bertorello C, Rinauro B, Sannino G, Bonfanti M, et al. Experimental validation of orcaflex-based numerical models for the PEWEC device. Ocean Eng 2023;281:114963.

[44] Pozzi N, Bracco G, Passione B, Sirigu SA, Mattiazzo G. PeWEC: Experimental validation of wave to PTO numerical model. Ocean Eng 2018;167:114–29.

[45] Giorcelli F, Sirigu SA, Pasta E, Gioia DG, Bonfanti M, Mattiazzo G. Wave energy converter optimal design under parameter uncertainty. In: International conference on offshore mechanics and arctic engineering, Vol. 85932. American Society of Mechanical Engineers; 2022, V008T09A085.

[46] Faltinsen O. Sea loads on ships and offshore structures, Vol. 1. Cambridge University Press; 1993.

[47] Paduano B, Parrinello L, Niosi F, Dell'Edera O, Sirigu SA, Faedo N, et al. Towards standardised design of wave energy converters: A high-fidelity modelling approach. Renew Energy 2024;224:120141.

[48] Folley M. Numerical modelling of wave energy converters: State-of-the-art techniques for single devices and arrays. Academic Press; 2016.

[49] Babarit A, Delhommeau G. Theoretical and numerical aspects of the open source BEM solver NEMOH. In: 11th European wave and tidal energy conference. 2015.

[50] Gioia DG, Pasta E, Brandimarte P, Mattiazzo G. Data-driven control of a pendulum wave energy converter: A gaussian process regression approach. Ocean Eng 2022;253:111191.

[51] Pecher A, Kofoed JP. Handbook of ocean wave energy. Springer Nature; 2017.

[52] Hasselmann K, Barnett TP, Bouws E, Carlson H, Cartwright DE, Enke K, et al. Measurements of wind-wave growth and swell decay during the joint North sea wave project (JONSWAP). Ergaenz Dtsch Hydrogr Z Reihe A 1973.

[53] Borretta E, Giglio E, Luzzani G, Terranova V, Trivigno G, Niccolai A, et al. Software-based solutions for the optimization of a building electric bill using integrated PV and storage systems: A case study. In: 2021 IEEE international conference on environment and electrical engineering and 2021 IEEE industrial and commercial power systems europe (EEEIC/i&cPS europe). IEEE; 2021, p. 1–6.
[54] Guanche R, De Andres A, Simal P, Vidal C, Losada I. Uncertainty analysis of wave energy farms financial indicators. Renew Energy 2014;68:570–80.
[55] De Andres A, Medina-Lopez E, Crooks D, Roberts O, Jeffrey H. On the reversed LCOE calculation: Design constraints for wave energy commercialization. Int J Mar Energy 2017;18:88–108.
[56] Ambühl S, Marquis L, Kofoed JP, Dalsgaard Sørensen J. Operation and maintenance strategies for wave energy converters. Proc Inst Mech Eng Part O: J Risk Reliab 2015;229(5):417–41.
[57] Guanche R, De Andrés A, Losada I, Vidal C. A global analysis of the operation and maintenance role on the placing of wave energy farms. Energy Convers Manage 2015;106:440–56.
[58] De Andres A, Maillet J, Hals Todalshaug J, Möller P, Bould D, Jeffrey H. Techno-economic related metrics for a wave energy converters feasibility assessment. Sustainability 2016;8(11):1109.
[59] O'Connor M, Lewis T, Dalton G. Operational expenditure costs for wave energy projects and impacts on financial returns. Renew Energy 2013;50:1119–31.
[60] Chang G, Jones CA, Roberts JD, Neary VS. A comprehensive evaluation of factors affecting the levelized cost of wave energy conversion projects. Renew Energy 2018;127:344–54.
[61] Lavidas G, Blok K. Shifting wave energy perceptions: The case for wave energy converter (WEC) feasibility at milder resources. Renew Energy 2021;170:1143–55.
[62] Ocean Energy Europe. 2030 ocean energy vision. 2020, URL https://www.oceanenergy-europe.eu/wp-content/uploads/2020/10/OEE_2030_Ocean_Energy_Vision.pdf. [Accessed 21 November 2024].
[63] Sandia National Laboratiries. Technological cost-reduction pathways for attenuator wave energy converters in the marine hydrokinetic environment. 2013, URL https://www.osti.gov/servlets/purl/1096511. [Accessed 21 November 2024].
[64] United States Department of Energy - Wind & Water Power Technologies Program. The future potential of wave power in the United States. 2012, URL https://www.ourenergypolicy.org/wp-content/uploads/2012/10/The-Future-of-Wave-Power-MP-9-20-12.pdf. [Accessed 21 November 2024].
[65] MacGillivray A, Jeffrey H, Winskel M, Bryden I. Innovation and cost reduction for marine renewable energy: A learning investment sensitivity analysis. Technol Forecast Soc Change 2014;87:108–24.
[66] ETRI E. Energy technology reference indicator projections for 2010–2050. Jt Res Cent Eur Comm 2014.
[67] Ringwood JV, Zhan S, Faedo N. Empowering wave energy with control technology: Possibilities and pitfalls. Annu Rev Control 2023;55:18–44.
[68] Papini G, Pasta E, Carapellese F, Bonfanti M. Energy-maximising model predictive control for a multi degree-of-freedom pendulum-based wave energy system. IFAC-Pap 2022;55(31):433–8.
[69] Brown T, Hörsch J, Schlachtberger D. Pypsa: Python for power system analysis. J Open Res Softw 2018;6(4). http://dx.doi.org/10.5334/jors.188, arXiv:1707.09913.
[70] Moscoloni C, Zarra F, Novo R, Giglio E, Vargiu A, Mutani G, et al. Wind turbines and rooftop photovoltaic technical potential assessment: Application to sicilian minor Islands. Energies 2022;15(15). http://dx.doi.org/10.3390/en15155548, URL https://www.mdpi.com/1996-1073/15/15/5548.
[71] Rozzi E, Giglio E, Moscoloni C, Novo R, Mattiazzo G, Lanzini A. Comparative study of electric and hydrogen mobility infrastructures for sustainable public transport: A PyPSA optimization for a remote island context. Int J Hydrog Energy 2024;80:516–27. http://dx.doi.org/10.1016/j.ijhydene.2024.07.105, URL https://www.sciencedirect.com/science/article/pii/S0360319924027769.
[72] Muñoz-Sabater J, Dutra E, Agustí-Panareda A, Albergel C, Arduini G, Balsamo G, et al. ERA5-land: A state-of-the-art global reanalysis dataset for land applications. Earth Syst Sci Data 2021;13(9):4349–83.
[73] Coe RG, Ahn S, Neary VS, Kobos PH, Bacelli G. Maybe less is more: Considering capacity factor, saturation, variability, and filtering effects of wave energy devices. Appl Energy 2021;291:116763.
[74] Davidson J, Nava V. Targeting the high frequency tail of wave spectra for energy harvesting in marine sensor networks. 2024, Available At SSRN 4758518.